NASA TECHNICAL MEMORANDUM

NASA TM X-1334

NASA TM X-1334

GPO PRICE $ ______

CFSTI PRICE(S) $ ______

Hard copy (HC) ______

Microfiche (MF) ______

ff 653 July 65

FACILITY FORM 602

(ACCESSION NUMBER)	(THRU)
71 (PAGES)	(CODE)
TMX-1334 (NASA CR OR TMX OR AD NUMBER)	30 (CATEGORY)

PAYLOAD TO MARS RECONNAISSANCE ORBIT USING PRESENT AND FUTURE BOOSTER SYSTEMS

by C. A. Wagner

Goddard Space Flight Center
Greenbelt, Md.

NATIONAL AERONAUTICS AND SPACE ADMINISTRATION • WASHINGTON, D. C. • FEBRUARY 1967

NASA TM X-1334

PAYLOAD TO MARS RECONNAISSANCE ORBIT USING PRESENT AND FUTURE BOOSTER SYSTEMS

By C. A. Wagner

Goddard Space Flight Center
Greenbelt, Md.

NATIONAL AERONAUTICS AND SPACE ADMINISTRATION

For sale by the Clearinghouse for Federal Scientific and Technical Information
Springfield, Virginia 22151 – Price $2.50

ABSTRACT

This report derives and illustrates a simple method by which deliverable payload to specified space missions can be calculated, utilizing arbitrary boosters and upper stage systems.

Using this method, a number of booster and upper stage systems are examined for their capability of placing useful payloads into Mars orbit in the period 1966-1969. It is found that with present operational systems, payloads of 100-300 pounds may be placed in favorable orbits for continuously observing conditions on and near Mars and the near vicinity and relaying this information back to earth. By using boosters and a Mars stage of a conventional chemical or radioisotope powered engine, which may be operational in the years 1966-1967, it is feasible to deliver payloads of 350-1000 pounds into favorable Mars orbits. For the years 1966-1969 operational boosters in the Titan III class matched to a Mars stage consisting of a conventional solid or bipropellant engine, and/or a near-future radioisotope-powered engine, will be capable of placing 1000-2300-pound payloads into a Mars reconnaissance orbit.

In particular, for 1966 launch dates, using a booster in the Titan II/Agena D or Atlas/Centaur Class, it is estimated that a Mars sensor payload of 150 pounds, consisting of about 30 percent of the EGO (Eccentric Orbiting Geophysical Observatory) experiment package and two Nimbus low-resolution TV cameras, can be placed into a favorable Mars reconnaissance orbit. The Mars spacecraft carrying and controlling this payload could be built around existing Mariner and/or EGO hardware for an operating lifetime in Mars orbit on the order of two years or the period between two Earth-Mars oppositions.

Preliminary comparison of performance capabilities of low-thrust, radioactively powered versus conventional chemical Mars stage propulsion systems indicates that the low thrust-high performance systems offer little, if any, payload advantage for Mars orbiter spacecraft of 500 pounds or less. However, using a Titan II/Agena D booster, a two or three-stage, low-thrust system employing a high-thrust Mars injection engine, could place 800-1000 pounds in a favorable eccentric Mars orbit with a synchronous period and a minimum altitude of 1000 kilometers, compared with 650-800 pounds for a one-stage chemical system into the same orbit with the same initial booster. The maximum achievable payload into this favorable orbit with a *single* low-thrust Mars stage and the Titan II/Agena D or Centaur boosters appears to be only 400-540 pounds.

CONTENTS

PAYLOAD TO MARS RECONNAISSANCE ORBIT USING PRESENT AND FUTURE BOOSTER SYSTEMS

by
C. A. Wagner
Goddard Space Flight Center

INTRODUCTION

There has been much interest in recent years in the possibility of placing heavy payloads in a Mars reconnaissance orbit for the purpose of a long term survey of that planet from close range (References 1 and 2). The objectives of this report are four. The first is to provide a simple method by which deliverable payload weights for specified missions can be calculated, and the payload results of using arbitrary booster and upper stage systems compared on an efficient, comprehensive basis. The other objectives are to indicate broadly (see Table 1): (a) the class of Mars orbiters which appear most promising for providing the greatest amount of useful information about that planet; (b) the reasonable payload weights which may be associated with them; and (c) the class of Mars orbiter missions which could favorably utilize a near-future, low-thrust-high performance rocket engine. In the course of this investigation it will be necessary to calculate in detail the characteristic velocities involved in the critical phases of various Mars orbiter missions, including those achievable by low-thrust, high-specific impulse upper stages.

In a later study, we hope to examine competitively low-thrust and high-thrust performance of the most promising Mars orbiter missions revealed in this study, considering fully realistic trajectories as well as detailed attitude control requirements for all phases of the mission.

The basic simplified technique of calculating mission payload weights used in this report is derived in an appendix from first principles. In Reference 1 this method was used in a reverse manner to that employed here, to estimate booster takeoff weights for a given payload in Mars orbit employing various booster and Mars stage systems. The problem of the optimum means of transferring to or from hyperbolic trajectories to or from circular orbits of a central body was first discussed by Lawden (Reference 3) and more recently, in greater detail, by Ehricke (Reference 4).

Table 1

Payload Weight (pounds) in Mars Orbit as a Function of Booster System, Mars Stage and Mission
Preliminary Estimates of the Stages of a Mars Orbit Mission.

Initial Booster System (Weight Range in Earth-Mars Transfer Trajectory)	One Mars Stage						Two Stages	Three Stages
	Solid (I_{sp} = 285 sec)				Poodle (I_{sp} = 750 sec)		Poodle (I_{sp} = 750 sec) with Solid (I_{sp} = 285 sec): Mars 24-hr Orbiter, Ec-centric Orbit, Apocenter Alt. = 33,000 km Pericenter Alt. = 1000 km	Poodle (I_{sp} = 750 sec) with Two Solid Stages (I_{sp} = 285 sec): Mars 24-hr Orbiter, Ec-centric Orbit, Apocenter Alt. = 33,000 km Pericenter Alt. = 1000 km
→	Mars "Nimbus" Orbiter, Circular Orbit, Altitude = 500 km	Mars "Low Alt. ATS" Orbiter, Circular Orbit, Altitude = 6000 km	Mars 24-hr Orbiter, Circular Orbit, Altitude = 17,000 km	Mars 24-hr Orbiter, Ec-centric Orbit, Apocenter Alt. = 33,000 km Pericenter Alt. = 1000 km	Mars 24-hr Orbiter, Circular Orbit, Altitude = 17,000 km	Mars 24-hr Orbiter Ec-centric Orbit, Apocenter Alt. = 33,000 km Pericenter Alt. = 1000 km		
Atlas-Agena D (350-500)	130-190 (H.1.3.A.)*	150-210 (H.1.3.B.)*	140-210 (H.1.3.C)*	230-320 (H.1.3.D.)*	0-60 (L.1.3.C.)*	33-118**		
Atlas-Centaur or Titan II/ Agena D (1000-1250)	380-480 (H.2.3.A.)*	420-530 (H.2.3.B.)*	420-520 (H.2.3.C.)*	650-820 (H.2.3.D.)*	280-390 (L.3.3.C.)*	400-541**		
Titan III-C (3000-3500)	1160-1350 (H.3.3.A.)*	1280-1500 (H.3.3.B.)*	1270-1480 (H.3.3.C.)*	1970-2300 (H.3.3.D.)*	1180-1410 (L.3.3.C.)*	1530-1812**		
Centaur (8800 # in Earth Orbit)							850**	1020**

NOTES: All numbers in this table are in pounds rounded off to the lowest 10 pounds to maintain a conservative estimate.
*See Table 3 for mission nomenclature and a full comparison of booster systems and missions employing a single Mars stage.
**See Appendix F.

At the start of the study, for the sake of simplicity and because it was felt the comparative results between low- and high-thrust operations would still be valid, the following idealizations and assumptions were imposed:

1. The Earth and Mars move in coplanar circular orbits about the sun.
2. Only single-stage Mars spacecraft would be considered.
3. Trajectory "touch-up" requirements during and after the Earth-Mars transfer phase would be negligible compared to the gross trajectory requirements calculated for the earth escape to Mars capture mission in any given case.
4. Attitude control velocity requirements could be considered separately from trajectory velocity requirements.

The limitations and penalities of the first assumption are discussed in some detail in Appendix E. In the later study the restrictions of this assumption will be removed altogether with the aid of exact Earth-Mars trajectory information supplied by the Lockheed Missile and Space Company and the Jet Propulsion Laboratory.

The third assumption appears strictly valid in this report, at least for the Mars transfer phase, for all missions which begin with the spacecraft in that nominal transfer Earth-Mars orbit. This is verified by noting that Mars-Mariner 1964 launched by an Atlas-Agena D weighed about 575 pounds including a midcourse (trajectory touch-up) motor which must have weighed about 50 pounds according to the original design weight for Mariner in Table D-1. This leaves a Mars-1964 spacecraft payload weight of about 525 pounds destined to pass within 6000 miles (9600 kilometers) of the surface of Mars according to JPL in December 1964, and without a second midcourse correction which it is capable of delivering. It is apparent that the maximum payload allotment of 500 pounds for this transfer, assigned to the Atlas-Agena D by the launch vehicle summary, (Reference 10) includes trajectory touch-up capability in an added midcourse motor sufficient to assure (depending, of course, on necessary guidance) Mars injection at any desired altitude above that planet.

After the study was well underway, considerations of the energy involved and the advantages of Mars observation from an eccentric Mars orbiter obviously precluded any but a high-thrust, single Mars stage in competition with low-thrust engines below an I_{sp} equal to about 1000 seconds, This being so, it seemed only fair to relax the second assumption in this part of the study and consider a combined low thrust-high thrust, two-stage Mars spacecraft which could as reasonably be relied upon to achieve this Mars orbit as a single, high-thrust stage.

In Appendix F it is shown, for example, that such a two-stage system will outperform by a small margin a single high-thrust Mars stage system in the achievement of this Mars orbit for launches in 1966/67. This performance is attributable in large part to the additional staging operation which should perform reliably at an intermediate-altitude earth orbit. However, it is also at least partially attributable to the efficiency of the low-thrust lifting which provides a higher platform from which to achieve the necessary earth-hyperbolic excess to reach Mars.

I. GENERAL CONSIDERATIONS OF MARS ORBIT MISSIONS

To place a payload from Earth in orbit about Mars, three distinct sub-missions must be accomplished to deal with the controlling gravity fields of first the Earth, then the Sun, and then Mars. The three submissions can be called: 1. Earth escape; 2. Earth-Mars transfer; 3. Mars capture. To accomplish each of these phases a certain amount of energy is required—energy that must be expended as fuel in a rocket engine which must be carried along with the payload. Obviously, the more energy required for a mission or submission, the less the deliverable payload at the end of the mission, since more rocket fuel and/or engine weight is required to accomplish it.

Instead of "mission energy" it has become conventional to speak of the "characteristic velocity" of a mission (see Appendix B), referring directly to the rocket engine which must accomplish it. "Characteristic mission velocity" in this report is the total velocity increment to the rocket-spacecraft which must be added by operation of the rocket engine after the start of the mission to place the payload in the desired trajectory or orbit. The relation between this characteristic velocity and the mass lost by the rocket (of a given initial mass) to achieve it is a function of the specific impulse of the rocket fuel only. The higher the specific impulse of the fuel, the less fuel mass need be expended by the rocket-spacecraft in achieving the characteristic velocity of the mission. The single quantity which expresses the relationship of lost mass to specific impulse and characteristic velocity is called the "mission parameter" M (see Figure 1).

If the characteristic velocity of a mission were always the same no matter what path was chosen to accomplish it, then it is obvious that, all other considerations aside, the higher impulse rocket engines are the engines of choice for the mission. Unfortunately, this is not the case; the combined forces of gravity and rocket thrust acting on the spacecraft during powered flight are not conservative. The general solution of the problem of finding the trajectory with the minimum energy requirements or the minimum characteristic velocity for a given interplanetary mission whose arbitrary end points are specified has not been found. However, we do know many special classes of optimum solutions where the powered-flight regimes are constrained in a manner allowing the realistic use of rocket hardware. In particular, there is the well-known class of Hohmann transfers between coplanar, circular orbits of a single central body which are optimum under the constraint of a two-impulse maneuver.

A. Low-Thrust Mars Orbiter Mission Profiles

In considering the mission profile of a spacecraft powered by a rocket engine of specific impulse much above that generated by the combustion of conventional chemical fuels, the chief constraints are generally low-thrust and long rocket "on times." By low thrust is meant thrust of at least an order of magnitude less than the controlling gravity force at a particular phase of the mission. For example, for operations close to the earth where the acceleration of gravity is of the order of magnitude of 1-10 ft/sec^2, the upper stage thrust to spacecraft weight ratio, T_e/W, must be less than about $1/32.15 = 0.031$ for the assumed low-thrust regime to be approximately valid. (The acceleration of W under the thrust T_e is given as $\ddot{S} = T_e\, g/W$, where W and T_e are in pounds and

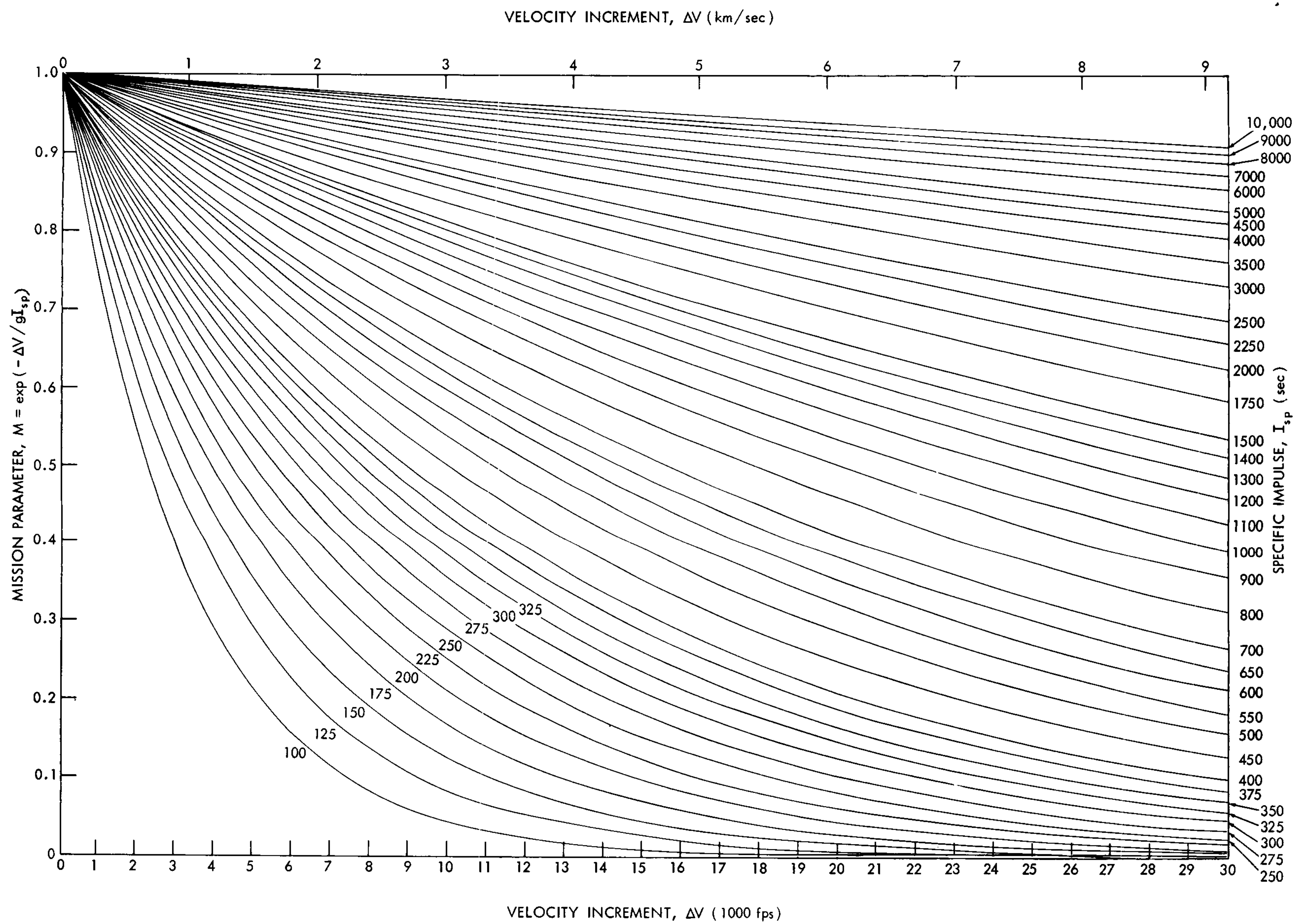

Figure 1—Mission parameter as a function of velocity increment, ΔV, and specific impulse, I_{sp}.

$g = 32.15$ ft/sec^2.) The low thruster examined in this study generates a thrust of the order of magnitude of 1 pound. Thus, the assumed low-thrust, "spiral" regime for operations in the vicinity of the earth will be approximately valid as long as spacecraft weight is of the order of 100 pounds in the vicinity of the earth. This is always the case for the favorable Mars missions (Table 1).

For operations in near-earth interplanetary space under the influence of solar gravity, the critical thrust-to-weight ratio is of the order of 1/10,000 pounds, as the acceleration due to the sun is of the order of $\mu_s/1$ AU $= 0.000296$ AU/day^2 $= 8.23 \times 10^{-3}$ ft/sec^2. Thus, for most of the "low thrust" Mars missions in this report, the interplanetary phase from Earth to Mars will follow a trajectory somewhere between a segment of a Hohmann ellipse and a close spiral. However, as shown in Appendix C, the pure Hohmann transfer between Earth and Mars orbits is only slightly more economical of velocity requirement than the pure low-thrust, close-spiral regime.

The actual low-thrust velocity requirement for the interplanetary phase of the complete low-thrust missions, 1 and 2 in Table 2, will be little different from that calculated for Table 2. In the vicinity of Mars, the gravity acceleration is of the order of

$$\frac{\mu_{\mathrm{Mars}}}{(5000\ \mathrm{km})^2} = \frac{0.429 \times 10^5\ \mathrm{km}^3/\mathrm{sec}^2}{25 \times 10^6\ \mathrm{km}^2} = 1.72 \times 10^{-3}\ \mathrm{km/sec}^2 = 5.64\ \mathrm{ft/sec}^2$$

Thus, the critical spacecraft weight for validity of the low-thrust, close-spiral regime requirements in the vicinity of Mars is, as in the case for near-earth operations, of the order of 100 pounds for the 1-pound thruster studied. Again, this requirement is met for the favorable low-thrust Mars mission spacecrafts of Tables 1 and 3. The low-thrust engine deadweight alone is 165 pounds for four 1/4-pound thrusters. Trajectories with such engines are gradually altered trajectories established at the beginning of a mission phase.

For a class of possible Mars orbit mission profiles which can utilize low-thrust trajectories, it has been found (Reference 1) that all of them yield characteristic velocities closely approximated by patching together pieces of gradually evolving spiral trajectories about first, the Earth, then the Sun, then Mars.

Table 2

Characteristic Velocities for Low-Thrust Mars Orbit Missions.

Boost Phase	Capture Phase for Mars Mission (circular orbits)	Mars Mission (total)	Characteristic Velocity (km/sec)
1. Low Earth Parking Orbit (300 n.m. altitude)	A. Mars-Nimbus orbiter (altitude: 500 km)	1.A.	16.61
		1.B.	15.44
		1.C.	14.75
2. Earth Escape	B. Mars-Low ATS orbiter (altitude: 6000 km)	2.A.	9.02
		2.B.	7.85
		2.C.	7.16
3. Earth-Mars Transfer Trajectory	C. Mars-synchronous orbiter (altitude: 17,000 km)	3.A.	5.91
		3.B.	4.74
		3.C.	4.05

Table 3

Deliverable Payload Weights for Various Boost-Mars Orbit Combinations.*

Mars Mission	Weight at the Start of Mission, W_0 (pounds)	Velocity Increment, ΔV (km/sec)	Specific Impulse, I_{sp} (sec)	Propellant Tankage Constant, C_T	Engine Dead Load Fraction, C_E	Mission Parameter, M	Payload Fraction, $(PL)_F$	Payload Wt. in Mars Orbit, W_{PL} (pounds)	Comments
L.1.1.A.	5900	16.61	750	0.3	0.028	0.104	-0.194	-1142	Not feasible with one Mars stage
L.1.2.A.	925	9.02	750	0.3	0.178	0.292	-0.097	-90	Not feasible with one Mars stage
L.1.3.A.	350-500	5.91	750	0.3	0.471-0.33	[0.446]	-0.192/0.050	-67/.25	Not feasible with one Mars stage
H.1.3.A.	350-500	2.06	285	0.177	0	0.479	0.386	135/193	See Table 1
L.2.1.A.	8800	16.61	750	0.3	0.019	0.104	-0.185	-1624	Not feasible with one Mars stage
L.2.2.A.	2250	9.02	750	0.3	0.073	0.292	0.007	16	Compare with L.2.3.A. & H.2.3.A.
L.2.3.A.	1000-1250	5.91	750	0.3	0.165-0.132	[0.446]	0.116/0.149	116/186	Compare with H.2.3.A.
H.2.3.A.	1000-1250	2.06	285	0.177	0	0.479	0.386	386/483	See Table 1
L.3.1.A.	23,000	16.61	750	0.3	0.007	0.104	-0.172	-3950	Not feasible with one Mars stage
L.3.2.A.	5000	9.02	750	0.3	0.033	0.292	0.047	235	Compare with L.3.3.A. & H.3.3.A.
L.3.3.A.	3000-3500	5.91	750	0.3	0.055-0.047	[0.446]	0.226/0.234	679/820	Compare with L.3.3.A. & H.3.3.A.
H.3.3.A.	3000-3500	2.06	285	0.177	0	0.479	0.386	1160/1350	See Table 1
L.1.1.B.	5900	15.44	750	0.3	0.028	0.122	-0.168	-0.992	Not feasible with one Mars stage
L.1.2.B.	925	7.85	750	0.3	0.178	0.343	-0.031	-0.29	Not feasible with one Mars stage
L.1.3.B.	350-500	4.74	750	0.3	0.471-0.33	[0.525]	-0.089/0.054	-31/27	Compare with H.1.3.B.
H.1.3.B.	350-500	1.85	285	0.177	0	0.515	0.428	150/214	See Table 1
L.2.1.B.	8800	15.44	750	0.3	0.019	0.122	-0.160	-1414	Not feasible with one Mars stage
L.2.2.B.	2250	7.85	750	0.3	0.073	0.343	0.073	164	Compare with L.2.3.B. & H.2.3.B.
L.2.3.B.	1000-1250	4.74	750	0.3	0.165-0.132	[0.525]	0.218/0.251	218/314	Compare with H.2.3.B.
H.2.3.B.	1000-1250	1.85	285	0.177	0	0.515	0.428	428/535	See Table 1
L.3.1.B.	23,000	15.44	750	0.3	0.007	0.122	-0.188	-3400	Not feasible with one Mars stage
L.3.2.B.	5000	7.85	750	0.3	0.003	0.343	0.113	565	Compare with L.3.3.B. & H.3.3.B.
L.3.3.B.	3000-3500	4.74	750	0.3	0.055-0.047	[0.525]	0.328/0.336	985/1180	Compare with H.3.3.B.
H.3.3.B.	3000-3500	1.85	285	0.177	0	0.515	0.428	1285/1500	See Table 1
L.1.1.C.	5900	14.75	750	0.3	0.028	0.133	-0.168	-992	Not feasible with one Mars stage
L.1.2.C.	925	7.16	750	0.3	0.178	0.376	0.012	11	Compare with L.1.3.C. & H.1.3.C.
L.1.3.C.	350-500	4.05	750	0.3	0.471-0.33	[0.576]	-0.021/0.120	-7/60	See Table 1
H.1.3.C.	350-500	1.88	285	0.177	0	0.510	0.423	148/212	See Table 1
L.2.1.C.	8800	14.75	750	0.3	0.019	0.133	-0.146	-1284	Not feasible with one Mars stage
L.2.2.C.	2250	7.16	750	0.3	0.073	0.376	0.116	261	Compare with L.2.3.C. & H.2.3.C.
L.2.3.C.	1000-1250	4.05	750	0.3	0.165-0.132	[0.576]	0.285/0.318	285/398	See Table 1
H.2.3.C.	1000-1250	1.88	285	0.177	0	0.510	0.423	423/529	See Table 1
L.3.1.C.	23,000	14.75	750	0.3	0.007	0.133	-0.134	-3080	Not feasible with one Mars stage
L.3.2.C.	5000	7.16	750	0.3	0.033	0.376	0.156	780	Compare with L.3.3.C. & H.3.3.C.
L.3.3.C.	3000-3500	4.05	750	0.3	0.055-0.047	[0.576]	0.395/0.403	1185/1410	See Table 1
H.3.3.C.	3000-3500	1.88	285	0.177	0	0.510	0.423	1270/1480	See Table 1
H.1.3.D.	350-500	0.95	285	0.177	0	0.711	0.659	231/329	See Table 1
H.2.3.D.	1000-1250	0.95	285	0.177	0	0.711	0.659	659/823	See Table 1
H.3.3.D.	3000-3500	0.95	285	0.177	0	0.711	0.659	1975/2305	See Table 1

*An example of notation would be L.1.2.A. which refers to a low thrust mission, L (H indicates high thrust mission), using booster 1, boost phase 2, for Mars orbit A. Table 2 gives the nomenclature for booster, boost phase, and Mars orbit notation.

All of these profiles (as will be shown shortly) yield characteristic velocities in excess of those required to achieve the same Mars circular orbit by means or high-thrust, large-change maneuvers.

The great penalities of the low-thrust trajectories are to be found at the very beginning and at the very ends of the total mission. In the earth-escape phase, the low-thrust mission must begin from an earth parking orbit and, to give reasonable transfer times, the continuously thrusting rocket must move the spacecraft on an escape spiral. In contrast, the high-thrust rocket can achieve not only earth escape, but, with proper guidance, an Earth-Mars transfer trajectory by a single thrust from the earth's surface or from a low momentary parking orbit. There is always a weight penalty incurred when fuel must be carried against the pull of gravity before being burned.

Figure 2A and 2B contrast the mission profiles for placing a payload into a circular Mars orbit via high-thrust or low-thrust upper stage boosting. It is noted that the low-thrust mission is of the order of twice as long as the high-thrust. At the Mars capture end of the low-thrust mission, the relative velocity of the spacecraft must be low with respect to the planet. This is to allow sufficient time for the controlled in-spiralling, continuous thrust maneuver to take place in the vicinity of Mars encounter (Figure 2B).

Again this constraint on the low-thrust mission is wasteful of fuel since in effecting a capture it is generally best to burn the fuel as close to the planet as possible when the speed of the spacecraft is greatest, and when a given ΔV from the rocket effects the largest change of trajectory energy.* Some of these broad mission energy principles are discussed in greater detail in Appendices A and C. We can simply state here that the studies in Reference 5 showed that for continuous, low-thrust, circumferential thrusting, the characteristic velocity of a mission phase was very nearly equal to the circular velocity difference between the initial and final orbits. By circular velocity is meant the orbital velocity the spacecraft would have if the radial distance from the planet is always equal to its semimajor axis (see Discussion).

For the conservative calculations in this cursory investigation, we will assume that the end orbits of all low-thrust mission phases are perfectly circular. This being the case, the characteristic velocity for the complete low-thrust mission is the sum of:

1. $V_c\,(\text{Earth})_{\text{parking}}$, the circular velocity in the initial Earth-parking orbit;
2. $-V_c\,(\text{Mars})_{\text{solar}} + V_c\,(\text{Earth})_{\text{solar}}$, the difference in the circular velocities for Mars and Earth about the sun; and
3. $V_c\,(\text{Mars})_{\text{orbit}}$, the circular velocity in the final Mars reconnaissance orbit (see Table 2 and Figure 2B).

However, we can imagine two other partial low-thrust Mars mission profiles which utilize initial high thrusting to escape the earth. It will be instructive to compare the deliverable weights for these as an example of the gains for light spacecraft which can be realized by escape thrusting

*The high I_{SP}-low thrust spacecraft engine utilizing cryogenically stored propellant (i.e. the "poodle system") also suffers from excessively high tankage dead weight. This contributes to its poor comparative performance for delivering light payloads.

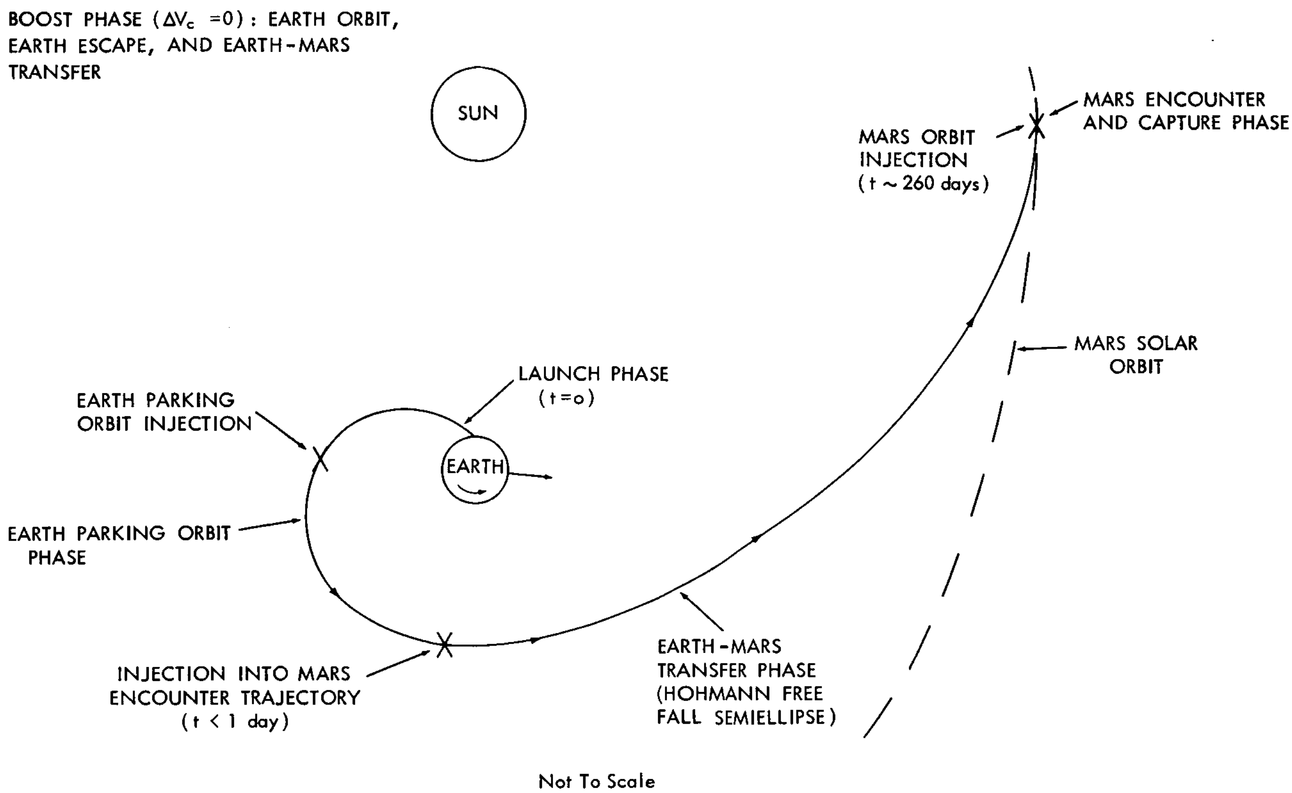

$\Delta V_c \equiv$ CHARACTERISTIC VELOCITY OR VELOCITY INCREMENT REQUIRED OF MARS STAGE ENGINE

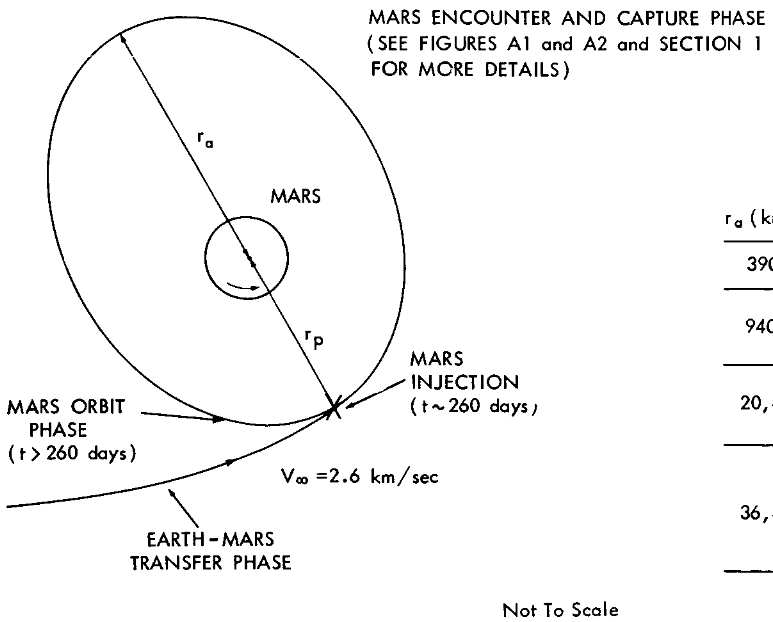

MISSION PROFILE DATA*

r_a (km)	r_p (km)	MARS ORBITER	$\Delta V_c \left(\frac{km}{sec}\right)$
3900	3900	NIMBUS (500 km alt.)	2.06
9400	9400	LOW ATS (6000 km alt.)	1.85
20,400	20,400	SYNCHRONOUS (17,000 km alt.)	1.88
36,400	4,400	SYNCHRONOUS ECCENTRIC (1000 km minimum altitude)	0.95

* All Maneuvers Are One-Impulse

Figure 2A—High-thrust, circular Mars orbiter mission profile.

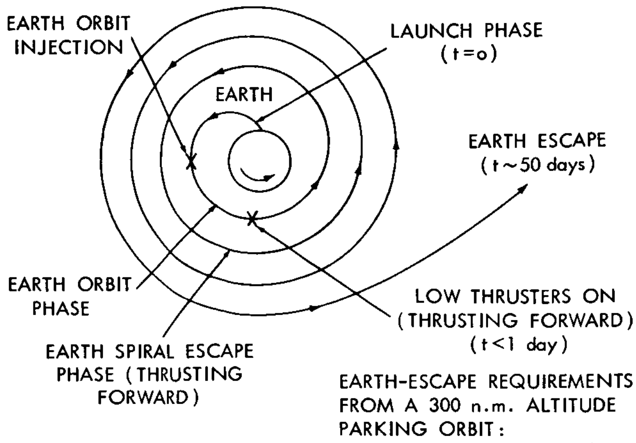

a. Boost Phase 1 - earth orbit

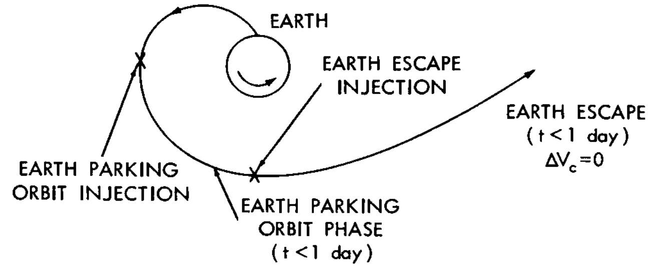

b. Boost Phase 2 - earth orbit and escape

(SEE FIGURE 2A FOR BOOST PHASE 3 - EARTH ORBIT AND ESCAPE PLUS EARTH-MARS TRANSFER)

$\Delta V_c \equiv$ CHARACTERISTIC VELOCITY OR VELOCITY INCREMENT REQUIRED OF MARS STAGE ENGINE

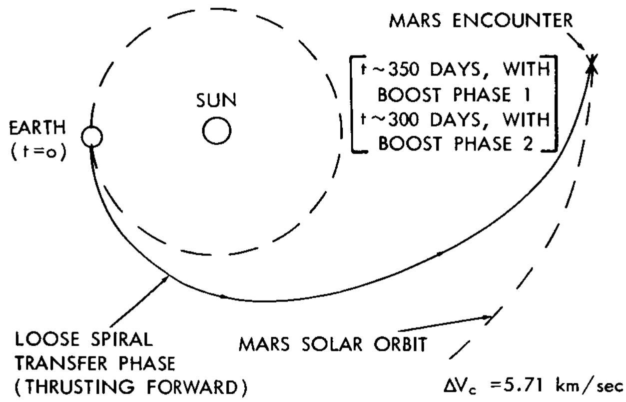

MARS TRANSFER PHASE THROUGH MARS ENCOUNTER WITH BOOST PHASES 1 and 2

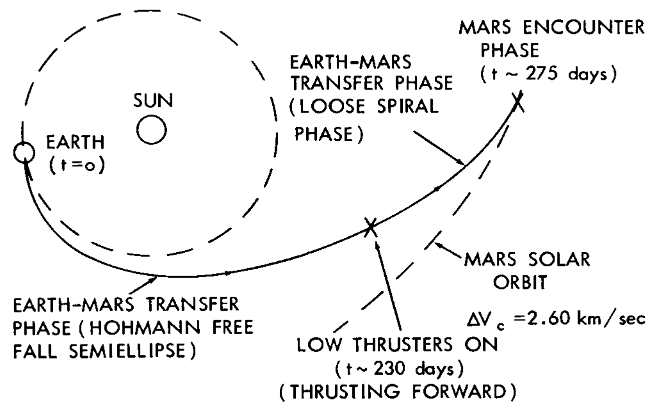

MARS TRANSFER PHASE THROUGH MARS ENCOUNTER WITH BOOST PHASE 3

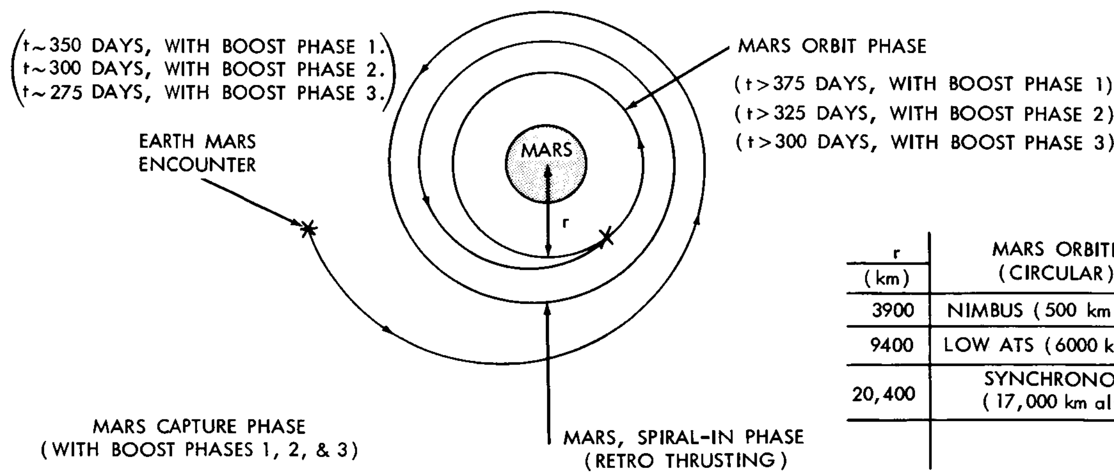

r (km)	MARS ORBITER (CIRCULAR)	ΔV_c (km/sec)
3900	NIMBUS (500 km alt.)	3.31
9400	LOW ATS (6000 km alt.)	2.14
20,400	SYNCHRONOUS (17,000 km alt.)	1.45
		(SEE TABLE 2)

Figure 2B—Low-thrust, circular Mars orbiter mission profiles close to the central body, even when the fuel burned is comparatively inefficient. In the first partial low-thrust profile, the booster puts the upper stage spacecraft into a barely earth-escape trajectory, whereupon the low-thrust upper stage completes the rest of the mission with a characteristic velocity which is the sum of velocities 2 and 3 above (Table 2 and Figure 2B). In the second partial low-thrust profile, the booster puts the upper stage spacecraft directly into an Earth-Mars transfer orbit, probably utilizing a low earth-parking orbit for adequate trajectory control.

In this mission, the low-thrust upper stage must adjust the aphelion velocity of the spacecraft trajectory so that, at Mars encounter (roughly 270 days after launch) the spacecraft is revolving around the sun at approximately the same rate as Mars. The velocity difference which must be made up is conservatively given as $V_c\,(\text{Mars})_{\text{solar}} - V(\text{unpowered Earth-Mars transfer orbit})_{\text{aphelion}}$, which, for the high-thrust upper stage missions, is the hyperbolic excess velocity $\left(V_\infty\,(\text{Mars})\right)$ for the Mars capture phase (see Discussion). To establish a typical value for V_∞, consider the Earth-Mars transfer trajectory ① in Figure 3.

In Figure 3 it is assumed that Mars is travelling around the sun in a circular orbit with a semimajor axis, $a_{\text{Mars}} = 1.524$ AU (the mean semimajor axis for 1960-1963 from Reference 6). The earth is assumed to be travelling around the sun in a circular orbit with a semimajor axis, $a_{\text{Earth}} = 1.000$ AU. The perihelion and aphelion of the elliptic transfer trajectory ① are thus

$$r_{p_①} = 1.000 \text{ AU}, \qquad r_{a_①} = 1.524 \text{ AU}.$$

The semimajor axis of trajectory ① is thus

$$a_① = \frac{1}{2}\left(r_{p_①} + r_{a_①}\right) = 1.262 \text{ AU}.$$

From the vis-viva integral of elliptic motion in a $1/r^2$ central field the velocity is (from Reference 7)

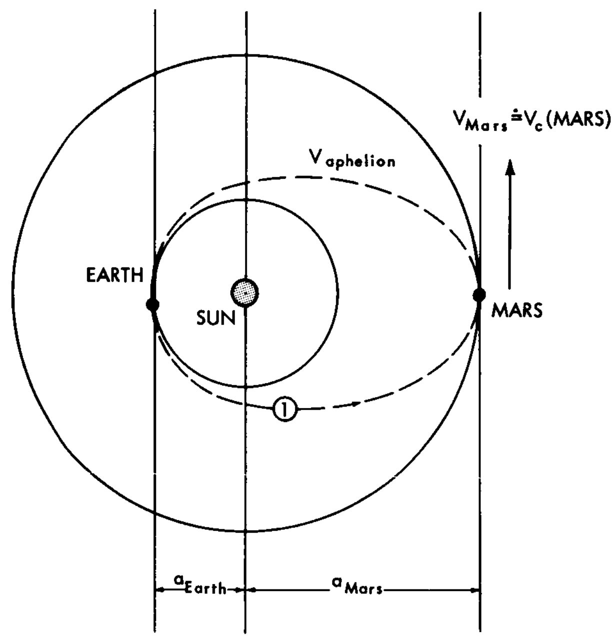

Figure 3—Earth-Mars transfer ellipse for Mars orbiter missions.

$$V = \left(\frac{\mu}{a}\right)^{1/2}\left[\frac{2a}{r} - 1\right]^{1/2} . \tag{1}$$

When Equation 1 is applied to the Earth-Mars transfer trajectory, the aphelion velocity is

$$V_{\text{aphelion}①} = \left(\frac{\mu_{\text{sun}}}{a_①}\right)^{1/2}\left[\frac{2a_①}{r_{a_①}} - 1\right]^{1/2}$$

$$= \left[\frac{\mu_{\text{sun}}}{1.262 \text{ AU}}\right]^{1/2}\left[\frac{2.524}{1.524} - 1\right]^{1/2}$$

$$= \left[\frac{\mu_{\text{sun}}}{1.262 \text{ AU}}\right]^{1/2}\left[0.810\right] .$$

According to Reference 6,

$$\mu_{sun} = 0.000296 \frac{AU^3}{(\text{solar day})^2} .$$

Therefore the aphelion velocity is

$$V_{aphelion①} = \left[\frac{0.000296}{1.262}\right]^{1/2} (0.810) = 0.0124 \frac{AU}{\text{solar day}} . \quad (2)$$

From Equation 1 with $r = a_{Mars}$, V_c (Mars) $\doteq V_{Mars}$ where

$$V_{Mars} = \left(\frac{\mu_{sun}}{a_{Mars}}\right)^{1/2} = \left(\frac{0.000296}{1.524}\right)^{1/2} = 0.0139 \frac{AU}{\text{solar day}} . \quad (3)$$

Thus the relative velocity of the spacecraft in the elliptical transfer trajectory with respect to Mars, at Mars encounter is, from Equations 2 and 3,

$$V_{\infty} = V_{Mars} - V_{aphelion①} = 0.0139 - 0.0124 = 0.0015 \frac{AU}{\text{solar day}} = 2.60 \frac{km}{sec} . \quad (4)$$

For the second partial low-thrust upper stage Mars orbiter mission, the characteristic velocity is then the sum of:

1. V_{∞} (Mars) = 2.60 km/sec
2. V_c (Mars)$_{orbit}$.

The remaining characteristic velocities for the low-thrust missions are V_c (Earth)$_{orbit}$, V_c (Mars)$_{orbit}$, and $-V_c$ (Mars)$_{solar}$ + V_c (Earth)$_{solar}$. A typical earth-parking orbit to start low-thrust operations on the spacecraft would be one at an altitude of about 300 nautical miles, as close to the earth as possible avoiding significant atmospheric drag. From Equation 1 with $r = a =$ (3440 n.m./earth radius + 300 n.m.) × 1.853 km/n.m. = 6935 km and $\mu_{earth} = 3.986 \times 10^5$ km^3/sec^2 (Reference 6), the orbital circular velocity at this altitude is

$$V_c (\text{low earth orbit}) = \left[\frac{3.986 \times 10^5}{6935}\right]^{1/2} = 7.59 \text{ km/sec} . \quad (5)$$

Three circular Mars reconnaissance orbits are chosen, two to give the same aspect of the planet Mars as the Nimbus and 600 nautical mile ATS earth orbits give of the planet earth, and the third to orbit with a period the same as the rotation period of Mars. For the special advantages of using this latter orbit, see page 14. The planet aspect ratio of the earth-Nimbus satellites (altitude = 500 n.m.) is given as r/r_{earth} = (500 n.m. + 3440 n.m.)/3440 n.m. = 1.146. Thus the equivalent Mars-Nimbus orbiter would have an orbit radius of $r = 1.146 \times r_{Mars} = 1.146 \times 3415$ km (Reference 6) = 3910 km. The Mars-Nimbus altitude would be 3910-3415 = 495 km. The circular velocity at this Mars radius would be

$$V_c \text{ (Mars-Nimbus orbiter)} = \left(\frac{\mu_{Mars}}{r_{Mars\text{-}Nimbus}}\right)^{1/2}$$

$$= \left[\frac{0.429 \times 10^5 \text{ km}^3/\text{sec}^2 \text{ (Ref. 6)}}{3910 \text{ km}}\right]^{1/2} = 3.31 \frac{\text{km}}{\text{sec}} \quad . \tag{6}$$

The planet aspect ratio of the 6000 nautical mile ATS satellite is given as

$$\frac{r}{r_{earth}} = \frac{6000 + 3440}{3440} = \frac{9440}{3440} = 2.74 \ .$$

Thus the equivalent Mars-low ATS orbiter would have an orbit radius of $r_{Mars\text{-}low\ ATS} = 2.74 \times 3415 = 9360$ km. (The altitude would be $\text{altitude}_{Mars\text{-}low\ ATS} = 9360\text{-}3415 = 5945$ km.)

The circular velocity at this Mars radius would be

$$V_c \text{ (Mars-low ATS orbiter)} = \left[\frac{0.429 \times 10^5}{9360}\right]^{1/2} = 2.14 \text{ km/sec} \ . \tag{7}$$

The rotation period of Mars is 24 hours, 37.4 minutes = 1477.4 minutes = 88,500 seconds (Reference 8). Since, from Kepler's third law, the period of a satellite T_s is given as a function of the semimajor axis by (Reference 7)

$$T_s = \frac{2\pi}{(\mu)^{1/2}} a^{3/2} \ ; \tag{7a}$$

the circular orbit radius for a Mars-synchronous satellite is

$$r_{Mars\text{-}sync.\ orbiter} = \left[\frac{88,500 \times (0.429 \times 10^5)^{1/2}}{2\pi}\right]^{2/3}$$

$$= 20,400 \text{ km} \ .$$

(The altitude would be

$$\text{altitude}_{Mars\text{-}sync.} = 20,400 - 3415 \cong 17,000 \text{ km.})$$

At this Mars radius the circular velocity would be

$$V_c\,(\text{Mars-sync. orbiter}) = \left[\frac{0.429 \times 10^5}{20,400}\right]^{1/2} = 1.45\,\text{km/sec.} \tag{8}$$

Finally, in those low-thrust missions where a spiral trajectory from Earth to Mars is necessary (following the earth-escape phase), a typical value of $V_c\,(\text{earth})_{\text{solar}}$ is required. From Equation 1 with $r = a \approx 1$ AU and $\mu = \mu_{\text{sun}}$

$$V_c\,(\text{earth})_{\text{solar}} = \left[\frac{0.000296}{1.0}\right]^{1/2} 0.0172\ \text{AU/solar day.} \tag{9}$$

The characteristic velocity which must be made up in the complete spiral Earth-Mars transfer part of the low-thrust mission is, from Equations 9 and 3,

$$V_c\,(\text{earth})_{\text{solar}} - V_c\,(\text{Mars})_{\text{solar}} = 0.0172 - 0.0139 = 0.0033\,\frac{\text{AU}}{\text{solar day}} = 5.71\,\text{km/sec.} \tag{10}$$

In summary, with the results of Equations 4, 5, 6, 7, 8 and 10, the characteristic velocities which must be made up by the low-thrust rocket engine of the upper stage spacecraft for typical Mars orbiter missions are to be found in Table 2 (see also Figure 2B).

B. High-Thrust Mars Orbiter Mission Profiles

The class of probable low-energy trajectories for the Mars orbiter mission utilizing a high-thrust upper stage engine is quite restricted when one places as a constraint that the engine can only be fired a limited number of times (Figure 2A). For maximum payload in the Earth-Mars transfer trajectory, with a reasonable control of the trajectory error, the boost phase will include the use of a low earth parking orbit. If a restartable liquid engine is used as the upper stage, it may be possible to use this to correct major trajectory errors midcourse to Mars. Otherwise secondary rockets must be provided with sufficient impulse capacity to effect any necessary gross trajectory adjustments. If a solid propellant rocket upper stage is chosen, then it still may prove feasible to utilize the small onboard attitude control jets or rockets to effect these adjustments if they are not too severe, at a weight saving. Additional weight saving may be possible with these high-thrust missions if these latter rockets are powered by a radioactively heated, cryogenically stored gas of low molecular weight, such as in the "Poodle System" (section II).

Instead of radiating away the excess heat in this latter rocket system, it may be possible to utilize much of it to power a good portion or all of the spacecraft-earth communications link when the attitude-trajectory control rockets are not firing (Discussion and Conclusions).

The capture phase of the high-thrust mission permits an economical achievement of a wide class of Mars orbits in the relatively short time of the Mars encounter. In Appendix A a general comparison is made of the velocity requirements of two-impulse against one-impulse Mars captures into a given circular orbit with a given hyperbolic excess. For the class of relatively close-circular orbits contemplated for the reconnaissance orbiter, it is found that the one-impulse capture is most efficient. For the circular, synchronous Mars orbiter, while the two-impulse capture is slightly more efficient in velocity requirement, the one-impulse maneuver is to be preferred for these early Mars missions as being far less complicated to execute and requiring only a single solid-stage burn (if a solid upper stage is chosen for the mission) (Appendix A).

C. Mars Eccentric Orbiter

If attitude control requirements are not excessive, capture velocity increments into an eccentric Mars orbit are considerably reduced over those for circular orbits of the same closest approach distance. An eccentric Mars orbiter also permits radial sampling of any Mars radiation belt or magnetic field. Observations of Mars taken near closest approach may be stored on tape for transmission to Earth at a more favorable point in the orbit.

The velocity requirements for a simple one-impulse eccentric capture at pericenter are just those given by Equation A15 in Appendix A for the first part of the two-impulse circular capture. These requirements are plotted in Figure 4 for minimum Mars approach altitudes of 0 and 1000 km. A particularly favorable semimajor axis for the Mars eccentric orbiter might be around 20,000 km where the period is close to 24 hours and near-synchronous for both Mars and Earth. With this orbit, favorable Earth transmission windows from a given geographic station could occur daily (at the Mars orbiter's apocenter) over an extended period of time. Conversely, only a small adjustment in the Mars orbit semimajor axis would be required to give a reasonably rapid drift rate of the satellite with respect to Mars. This would facilitate a complete circumferential coverage of the planet's surface (in the period of favorable earth transmission) taken by onboard monitors in the vicinity of pericenter. For a Mars pericenter altitude of 1000 km, excellent coverage of the near-Mars environment can be achieved with considerable weight savings over one-or two-impulse circular captures at either altitude (Section 2 and Figure 4).

Two other distinctly advantageous features of the eccentric Mars reconnaissance orbiter can be noted. It may be possible to gain valuable comprehensive information on the largely unknown density profile of the Martian atmosphere, without much risk to mission life with such an orbit, that would be impossible or difficult otherwise. For example, suppose a pericenter altitude of 1000 km is chosen for the orbiter on the basis of a nominal Martian atmospheric density profile. Now suppose the Martian atmosphere actually turns out to be many times more dense than nominall designed for. If the reconnaissance orbit were circular, the decay would be rapid as the satellite would lose about the same amount of energy to the atmosphere at all arguments in its orbit. But if the orbit is reasonably eccentric, the altitude decay will be considerably slower with a long initial period of orbit circularization at roughly a constant pericenter altitude. This behavior stems from the fact that the atmospheric density falls off rapidly with altitude, so that the effect of its drag on the orbit is initially felt only in the immediate vicinity of pericenter (Reference 4). During the long orbit-circularization period, accumulated observations on the decay of both apocenter and

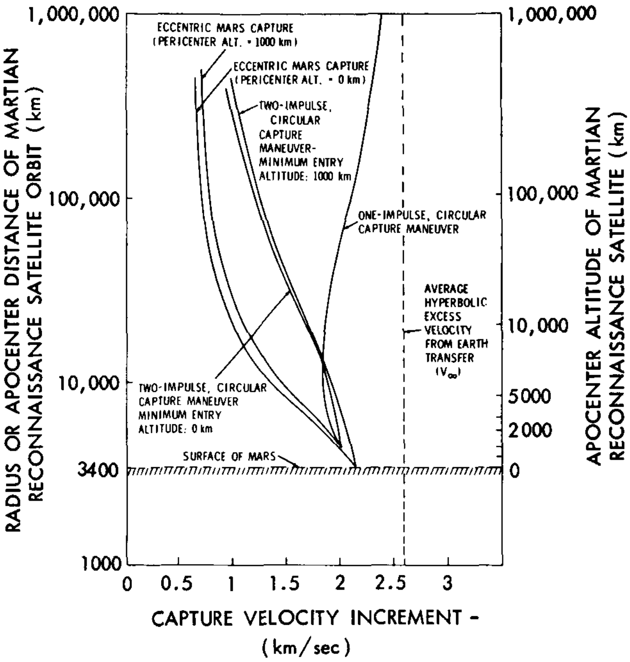

Figure 4—Capture velocity requirements for the high-thrust upper stage of a Mars reconnaissance orbiter.

pericenter with respect to Mars can be used to reconstruct a density profile of the planet for altitudes above about 1000 km, or the minimum chosen on the basis of the nominal design.

Another advantage of the eccentric orbiter whose pericenter is well defined is that it provides a convenient way to take stereo pictures of the surface of Mars. By utilizing one or two cameras shooting at symmetric planetary aspects around pericenter, information on the Martian topography (unobtainable in any other way because of the lack of sharp surface features on the planet) can be easily interpreted from the reconstructed picture information. The technique would require a close attitude control of the local vertical around pericenter. But this would be necessary in any case for the efficient operation of other Mars monitors. A more detailed description of the orbit control in this technique is found in Reference 9.

D. Velocity Requirements for High-Thrust Mars Missions

From the analysis in Appendix A, Figure 4 gives the Mars capture velocity requirements for the high-thrust upper stage of a Mars reconnaissance orbiter.

Table 4 below lists high-thrust upper stage velocity requirements taken from Figure 4 which correspond to the low-thrust Mars missions of Table 2. Also included for comparison is the "synchronous" eccentric Mars capture requirement discussed in section I.D.

II. DELIVERABLE PAYLOAD TO VARIOUS MARS ORBITS WITH VARIOUS BOOSTER AND UPPER STAGE SYSTEMS

Let the spacecraft be defined as a combination of a rocket engine and a payload. As used in this report, the mission, as far as the spacecraft is concerned, begins at first rocket burn and ends at fuel burn-out. The characteristic velocity of the mission is taken to mean the velocity increment which would be added to the spacecraft in free space during the total burn time of the rocket.

Let the specific impulse of the fuel be I_{sp} in seconds and the total burn time be t in seconds. Then the relationships between the burn time, the weight of the spacecraft W, the thrust of the

Table 4

Characteristic Velocities for High-Thrust Mars Orbiter Missions.

Boost Phase	Mars Mission (Capture Phase)	Mars Mission (total)	Characteristic Velocity (km/sec)
3. Earth-Mars Transfer Trajectory	A. Mars-Nimbus Orbiter (circular) (altitude: 500 km)	3.A.	2.06
	B. Mars-Low ATS Orbiter (circular) (altitude: 6000 km)	3.B.	1.85
		3.C.	1.88 (one-impulse maneuver)
	C. Mars-Synchronous Orbiter (circular) (altitude: 17,000 km)	3.D.	0.95
	D. Mars-Synchronous Orbiter (eccentric) (pericenter altitude: 1000 km; apocenter altitude: 33,000 km)		

rocket engine, T_e (in pounds) and the characteristic velocity, Δv (or free space velocity increment), are derived in Appendix B as

$$W(\text{weight of the spacecraft}) = W_0\left[e^{-(\Delta v/g I_{sp})}\right], \tag{11}$$

and

$$t = \frac{W_0 I_{sp}}{T_e} \quad 1 - e^{-(\Delta v/g I_{sp})} , \tag{12}$$

where W_0 is the weight in pounds of the spacecraft at the start of the mission and g is the earth's surface gravity acceleration (32.15 ft/sec^2). With the above units, Δv must be expressed in units of ft/sec. Equations 11 and 12 assume ideal free space rocket performance, in particular, constant thrust and constant I_{sp} during burn times.

Let the following spacecraft mission weights and constants be given:

M = mission parameter $= e^{(-\Delta v/g I_{sp})}$ (Figure 1) (12a)

$W_{E,D}$ $\equiv$ rocket engine deadweight (independent of the amount of fuel supply) plus any other engine-only associated deadweight independent of the amount of fuel supply (i.e., engine power supply equipment)

$W_{E,T}$ $\equiv$ rocket engine and/or fuel tank weight (dependent on the amount of fuel supply) plus any other associated deadweight so dependent

$W_{S/C}$ = deadweight of the spacecraft support structure

C_s = structure constant or factor

C_T ≡ fuel tankage or engine constant or factor

$(PL)_F$ ≡ payload fraction

C_E ≡ engine deadload fraction

W_F ≡ weight of fuel burned in the mission

C_S and C_T are defined from $W_{s/c}$, W_F, $W_{E,T}$, and W_0 by

$$C_S = \frac{W_{s/c}}{W_0}$$

and

$$C_T = \frac{W_{E,T}}{W_F} \quad . \tag{13}$$

In addition, we define the deliverable payload at tne end of the mission by W_{PL}, where

$$W_{PL} = W_0 - W_F - W_{E,D} - W_{E,T} - W_{s/c} \quad . \tag{14}$$

But the fuel burned in the mission is

$$W_F = W_0 - W \; . \tag{15}$$

By combining Equations 11, 12a, 13, and 15, Equation 14 becomes

$$W_{PL} = W_0 \left[M\left(1 + C_T\right) - \left(C_T + C_S + \frac{W_{E,D}}{W_0}\right)\right] \quad . \tag{16}$$

We can also define the terms payload fraction, $(PL)_F \equiv W_{PL}/W_0$, and engine deadload fraction, or factor, $C_E = W_{E,D}/W_0$. With these latter definitions Equation 16 now takes the form

$$(PL)_F = M\left[1 + C_T\right] - \left[C_T + C_s + C_E\right] \tag{17}$$

(see Figure 5).

We can now proceed to calculate deliverable payload fractions to various Mars orbits with various upper stage rocket engines. To convert these fractions into payload weights (and also to calculate C_E) we need to know the spacecraft weight, W_0, at the start of the mission.

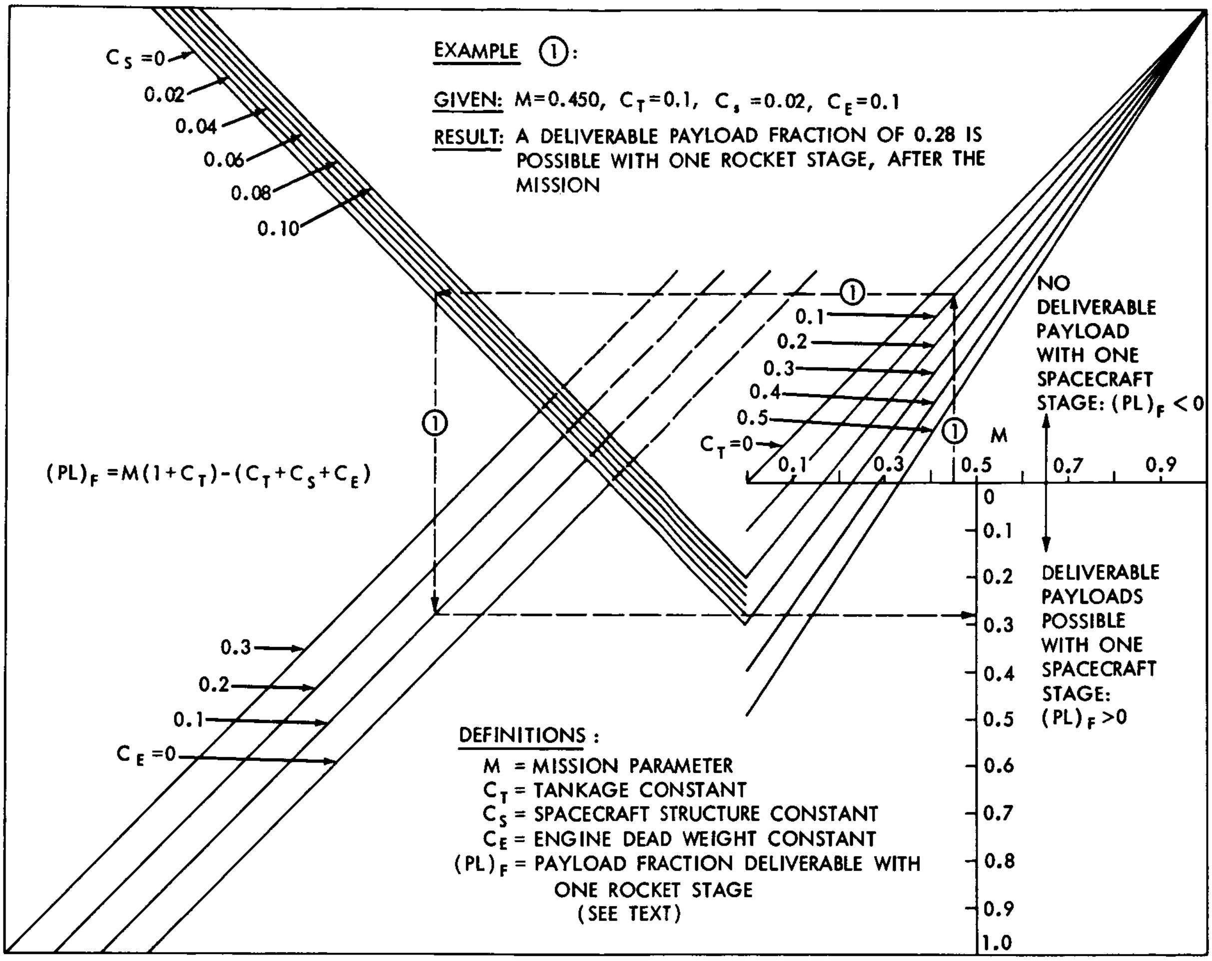

Figure 5—Deliverable payload fraction as a function of the mission and spacecraft parameters.

In the 1964 NASA-DOD launch vehicle summary (Reference 10) there is a range of velocity increment requirements listed from AMR (Atlantic Missile Range) for Venus and Mars fly-by missions, presumably in the next few decades. Payload weight in this range is assumed to be deliverable by the booster into the Earth-Mars transfer trajectory, a free fall heliocentric ellipse whose aphelion is at the distance of Mars from the sun at Mars-encounter. It is assumed that such a nominal trajectory will encounter Mars with a miss distance which will enable the high-thrust capture maneuvers to be executed as planned (Appendix A). In Tables 2 and 4, this booster trajectory is established as boost phase 3 of the various Mars missions.

To establish a reasonable order of magnitude for the Mars orbiter weight calculations in this report, two points in this range can be selected. The midpoint may be chosen to give the weight in the Earth-Mars transfer trajectory for a reasonably favorable launch window in *this* decade. To estimate the weight for the most favorable launch windows, the first quarter point of the ΔV range for Venus-Mars trajectories can be chosen. It is assumed that the first quarter of the range must be reserved for the lowest energy Venus fly-bys, since it can be shown that, starting from an Earth-escape trajectory, the Venus transfer requires less energy than the Mars. (The mean separation of Venus' orbit from Earth's is (1.0 - 0.723) = 0.277 AU (Reference 6). The mean separation of Mars' orbit from Earth's is (1.524 - 1.0) = 0.524 AU (Reference 6).)

Table 5 lists spacecraft weights, W_0, at the start of the Mars missions, after the boost phase, obtainable with various booster combinations. The meaning of the range of weights in missions with boost phase 3 is explained above (Reference 10).

Given below are the "ground rules" for the low-thrust and high-thrust Mars stage spacecraft:

Low-Thrust Mars Stage Spacecraft: The rocket system (called "poodle") which we consider is a hot gas thruster with radioactively heated cryogenically stored liquid hydrogen as the propellant. The I_{sp} is 750 seconds. The tankage constant (C_T) is 0.30. The engine deadweight ($W_{E,D}$) is 165 pounds (four thrusters giving a total engine thrust T_e = 1 pound)*. The spacecraft structure constant (C_S) is 0.02 (Reference 1).

High-Thrust Mars Stage Spacecraft: The rocket which we consider is a solid fuel rocket having the design specifications for the upper stage booster of the Advanced Technology Satellites (Reference 11). The I_{sp} is 285 seconds. The tankage constant (C_T) is 0.177. There is no engine deadweight independent of the amount of fuel supply. The spacecraft structure constant (C_s) is 0.02.

As an example of the Mars orbiter payload weight calculation, consider Mars mission L.3.1.C. (Table 4) defined as a low-thrust mission (L.) utilizing a Titan III-C boost (3) into a low earth orbit (1). The Mars orbit sought at the end of the mission is the circular synchronous one (C). From Table 1, the ΔV requirements for this mission are 14.25 km/sec. From Equation 12A or Figure 1, the mission parameter is $M = e^{-14.25\times 3281/32.15\times 750} = e^{-2.01} = 0.133$. The tankage constant C_T = 0.30. The spacecraft structure constant C_S = 0.02. The engine deadweight fraction is

Table 5
Initial Spacecraft Weights for Mars Missions.

Booster System	Boost Phase	Booster System Boost Phase	W_0 (Initial S/C Weight for Mars Mission) (pounds)
1. Atlas Agena D	1. Low earth parking orbit (300 n.m. altitude)	1.1	5900
2. Atlas/Centaur or Titan II/Agena D		1.2	925
	2. Earth Escape	1.3	350-500
		2.1	8800
	3. Earth-Mars Transfer Trajectory	2.2	2250
3. Titan III-C		2.3	1000-1250
		3.1	23,000
		3.2	5000
		3.3	3000-3500

*Low thrust engine constants (in the "poodle" system) supplied by Dennis Hasson of Goddard Space Flight Center.

$C_F = 165/23{,}000 = 0.00718$. From Equation 17, the deliverable payload fraction to Mars orbit is $(PL)_F = 0.133\,(1 + 0.3) - (0.3 + 0.02 + 0.00718) = -0.154$.

The conclusion is that this mission cannot be accomplished with a single upper stage spacecraft. Table 3 shows the relative efficiency of those feasible Mars mission profiles — the ones which can be accomplished with a single Mars rocket stage. While it would be possible to design a multistage Mars spacecraft which could accomplish any of the missions in Table 3, and with a weight efficiency greater than that calculated there, such a design would be less reliable than the single upper stage concept. The values in Table 3 for comparison between relative mission efficiencies would still hold for multistage execution of those missions. (See Appendix F for a discussion of a possible multistage chemical and exotic Mars orbiter mission.)

The most favorable missions in Table 3 are listed in Table 1.

III. MISSION TIME CONSIDERATIONS FOR MARS ORBITER MISSIONS

A. High-Thrust Mars Missions

Missions time for high-thrust upper stage Mars missions is controlled by the time in the Earth-Mars transfer ellipse (Figure 3). The semimajor axis of this minimum energy ellipse cotangent to both Mars and Earth solar orbits is about 1.26 AU (see page 11). From Reference 6 the gravitational constant of the sun is

$$\mu_s = 0.000296 \frac{AU^3}{(\text{solar day})^2} .$$

Thus, from Equation 7a, the time to Mars encounter from earth launch is about

$$\frac{T}{2} = \frac{\pi(1.26)^{3/2}}{(0.000296)^{1/2}} = 259 \text{ days.}$$

When the time spent in the Earth-parking orbit and in the Mars capture phase is counted, the execution time of the high-thrust Mars missions is of the order of 260 days.

B. Low-Thrust Mars Missions

For these missions gross time considerations will be more critical. The thrust design of the upper stage engines will depend, for the favorable missions, on the Earth-Mars trajectory time allowed for the spacecraft to achieve zero velocity with respect to Mars at Mars encounter. These missions (Table 3) begin with the spacecraft in a near-Hohmann semiellipse Earth-Mars transfer orbit. The velocity increment which must be made up in this phase of the mission is about 2.6 km/sec (Equation 4). Let us assume this velocity requirement, which holds strictly for all the thrust application at aphelion of the transfer ellipse, will be a good approximation of the requirement for near-Mars thrust on times of the order of one quarter of the 260 days spent in the semi-ellipse. Solving Equation 12 for T_e/W_0, the thrust-to-initial weight ratio, as a function of $M = e^{-\Delta/g I_{sp}}$, I_{sp}, and the engine "on" time t gives

$$\frac{T_e}{W_0} = \frac{I_{sp}}{t} (1 - M) \tag{18}$$

Equation 18, with $t = 260$ days/4 = 65 days = 56×10^5 sec, $\Delta V = 2.6$ km/sec and $I_{sp} = 750$ sec, becomes

$$\frac{T_e}{W_0} = 13.4 \times 10^{-5} (1 - 0.702) = 4.00 \times 10^{-5} \tag{19}$$

which is the requirement for timely execution of the interplanetary phase of the favorable low-thrust Mars mission.

The low-thrust missions which can realize appreciable payload weights in Mars orbits are those which utilize the Titan II/Agena D, Atlas/Centaur of Titan II-C for direct boost into the Earth-Mars transfer trajectory (Table 3). With the first two boosters, W_0 = 1000 - 1250 pounds. With the Titan III-C, W_0 = 3000 - 3500 pounds. Thus from Equation 19, for favorable missions with Titan II/Agena D or Atlas/Centaur boost, the minimum required upper stage engine thrust is

$$T_e \text{ (minimum)} = 1250 \times 4 \times 10^{-5} = 0.05 \text{ lb.}$$

For favorable missions with Titan III-C boost, the minimum required upper stage engine thrust is

$$T_e \text{ (minimum)} = 3500 \times 4 \times 10^{-5} = 0.14 \text{ lb.}$$

Thus, a gain in weight efficiency for these early low-thrust missions may be possible by utilizing a minimum 1/4-pound thruster Mars stage. For the worst case of the heaviest low-thrust Mars-Nimbus orbiter, the weight at Mars encounter is (from Equation 11) W_0 (Mars encounter) = 3500 $\times$ 0.702 = 2460 lb. The ΔV required to spiral into a 500 kilometer orbit altitude over Mars is 3.31 km/sec (Equation 6). The mission parameter for this last Mars orbiter mission phase is $M = 0.636$. From Equation 12, with $T_e = 0.25$ pounds, $W_0 = 2460$ pounds, $I_{sp} = 750$ sec, $M = 0.636$, this mission phase execution time is

$$t = \frac{24.60 \times 750}{0.25 \times 86,400 \text{ sec/day}} (1 - 0.636) = 31.1 \text{ days.}$$

Thus all the favorable low-thrust Mars missions can be executed in 260-290 days after Earth launch with a "minimum" engine thrust package. Whether it would be better to take this minimum thruster and save on engine deadweight, or take a number of thrusters to provide additional attitude and trajectory control on the way to Mars and in Mars orbit, will depend on detailed trade-off studies of these control requirements for the long-lived Mars orbiter mission (Discussion and Conclusions).

DISCUSSION

This report does not intend to provide a definitive answer to the question, "What is the most favorable Mars orbiter mission in the near future?" The intent is first to establish the broad basic ground rules by which realistic trajectory energy requirements for achieving a Mars orbit from earth launch can be calculated for low-thrust or high-thrust upper stage spacecraft systems. "Realistic" implies energy requirements which will be conservatively close to those which will actually be necessary for the Mars mission. The problem of the optimum trajectory is not discussed in any generality. However, the specific case of one- and two-impulse Mars capture trajectories under additional constraints believed to lead to minimal velocity requirements is analyzed in some detail and optimum regimes for these are established to achieve a wide class of Mars orbiters. What is approached throughout is a rational method for estimating favorable Mars orbiter payload weights utilizing Earth-Mars transfer trajectories that, while not optimum, will be not overly conservative either, when the mission is actually executed with near-future booster and upper stage systems.

As an example of the conservative nature of these calculations, consider the velocity requirements estimated for the "low thrust" Mars missions (Figure 2A). The actual trajectories in these missions will be opening or closing spirals and not almost perfectly circular as assumed. Low-thrust maneuvers involving planetary or interplanetary escape, capture, or transfer, can be made more efficient, the more strongly the original orbit or trajectory can be perturbed. A simple example of this is in planetary escape from a parking orbit of radius r. The velocity requirement for very low circumferential thrust escape (i.e., a close-spiral trajectory to an infinite distance from the planet) is just the circular velocity at r, $(\mu_p/r)^{1/2}$ (Reference 5). But the single impulse escape requirement is merely the "fall from infinity" velocity $(2\mu_p/r)^{1/2}$ minus $(\mu_p/r)^{1/2}$, or $0.414\,(\mu_p/r)^{1/2}$ which is 41.4 percent of the very low thrust requirement.

In particular, the greatest gain for the low thrust missions from this effect can be expected to occur for the favorable synchronous Mars orbiter missions of less than about 500 pounds, where operations will largely take place in the weak far-Mars gravity field under relatively large upper stage thrust-to-weight ratios. However, this gain is not expected to materially effect the weight comparisons in this report.

Additional conservatism for both high- and low-thrust regimes in this report (Figure 2) arises from the assumption that the Earth-Mars mission phase extends completely out to Mars before the Mars capture phase begins. Actually, these two phases begin to overlap roughly within a distance of the order of 100,000 miles from Mars as the planet's gravity field becomes dominant over the sun's. Again, these energy gains are expected to be small compared to the overall mission requirements.

It may be remarked here that calculations have shown that a bipropellant Mars stage ($I_{sp} \approx 300$ sec) with thrust of the order of magnitude of 250 pounds can provide about the same payload performance as the upper stage solid rocket assumed in the high thrust calculations. Such an engine, with a restart capability, would probably be able to achieve the desired Mars orbit with greater reliability than the single burn solid.

Again we note that only gross trajectory requirements have been compared in this study. The plane change requirements near Earth to place the spacecraft in a heliocentric orbit which actually encounters or comes close to Mars are assumed to be taken care of by the booster in boost phase 3 missions (Tables 2-5). The other low-thrust missions (boost phases 1 and 2) which have neglected this requirement are all less favorable than those with boost phase 3 to begin with. The velocity requirement for the plane change near Mars for these more complete low-thrust missions can be calculated to be of the order of 0.06 km/sec (see Appendix E), which is less than 1 percent of the total requirement for the least demanding of the missions (Table 2).

It may turn out that attitude and trajectory touch up control requirements for the long orbiter mission life will outweigh these gross energy considerations in the final choice of system components. The weight estimates made in this study are to be taken as a guideline or a base from which must be subtracted these additional control-propulsion requirements which will be different for each particular mission profile, to arrive at useful payload weights for the experiments and communications equipment in Mars orbit.

With regard to these additional propulsion requirements, it can be presumed that they can be bought most cheaply in weight by the use of the low-thrust, high-I_{sp} engine system with subsidiary fuel supplies. This is contrasted with using onboard, low-thrust, low-I_{sp} chemical or cold gas thrusters for these requirements. Against the advantage of high I_{sp}, the only weight penalty of the radioactive powered thruster for this task is the relatively large tankage weight necessary for shielding and insulation of the propellant. If the required attitude control torques are not too severe in the various phases of the mission, it may prove most favorable to utilize a number of low-thrust engines or an engine with multiple thrusters serving double duty for both trajectory and attitude control needs when the missions with heavier payloads become possible. Because of the large weight penalty of the radioactively powered engine deadload and tankage, this system only becomes feasible when these heavier boost loads are possible.

Another attractive feature of the radioactively powered system for the heavier Mars orbiter missions is the possibility for its otherwise wasted heat to serve as the primary source of power for the spacecraft-earth communications link (project "Snap-Poodle"). Power requirements for TV quality transmission over the long link to Mars will be high to begin with. They will be difficult to satisfy with solar arrays alone without a large weight penalty, at the distance of Mars from the sun (~1.54 AU).

Perhaps the chief difficulty in utilizing radioactively powered engines for the Mars orbiter mission is the lack of clearly suitable fissionable material. Plutonium 239 has an adequate half-life (of the order of thousands of years) but the yearly U.S. production will provide only 20 thermal kw, and this will just power a single "poodle" four 1/4-pound thruster stage. Polonium fuel is more readily available but the half-life is only 150 days. Conceivably one might use two radioactively powered engines in a two-stage, low-thrust, Mars spacecraft. One engine powered by polonium would handle the gross trajectory requirements on the way to Mars; the other, a two, 1/4-pound thruster stage powered by plutonium could handle the attitude propulsion requirements for the life of Mars orbiter mission, or share these with a chemical system. When Mars orbit is reached, the heavy polonium stage can be cut loose from the spacecraft to reduce attitude propulsion requirements for the life of the orbiter.

Unfortunately, none of these all-low-thrust Mars mission systems can be employed to achieve what appears to be the most favorable Mars eccentric orbiter mission. However, in view of its high I_{sp} and ability to serve as a subsidiary power supply, it may well prove advantageous to utilize a two or four, 1/4-pound thruster, plutonium-powered stage for the secondary (attitude and trajectory "touch up") propulsion requirements for the heavy eccentric orbiter missions. To accomplish attitude and trajectory control most efficiently at the Mars end, the "dead" solid or bipropellant "trajectory" stage should be jettisoned from the spacecraft in Mars orbit.

CONCLUSIONS

The need for obtaining high-quality, long-term scientific information about the planet Mars prior to a manned mission to that planet or for its own sake makes it attractive to consider the weight feasibility of a Mars orbiter mission in the near future (1965-1969). In particular it has been proposed that a radioactively powered low-thrust, high- I_{sp} rocket engine might offer unique advantages as the "Mars stage" of such a mission.

We conclude that while reasonably heavy payloads can be placed in favorable Mars orbits in the very near future (1965-1966) the single-stage, low-thrust radioactive engine proposed would probably be clearly superior only as a subsidiary trajectory and attitude control stage for the heavier orbiter missions in the years after 1966. The main factor in this judgment is the considerable energy savings which are possible with the choice of a highly eccentric Mars orbiter which, it appears, cannot efficiently be reached by a low-thrust stage alone. Such an orbit would also be particularly advantageous for obtaining comprehensive information about both the near and far Mars environment. However, if staging of the Mars spacecraft in earth orbit is allowed, mission profiles for the years after 1966 utilizing the low-thrust, high-performance engine for primary trajectory requirements become competitive with conventional chemical systems.

For example, we conclude that with operational boosters and upper stage systems presently available (1964), it is possible to place only 100-300 pounds of payload into a favorable Mars orbit. But by 1967, it may be feasible to place 1100-2300 pound payloads into this orbit. With such payloads, the use of the radioactive engine for at least subsidiary propulsion control purposes becomes competitive with conventional systems especially in view of the double-duty service such an engine can perform as a communications power supply. Detailed study of the attitude and trajectory control requirements for the Mars orbiter mission is warranted to confirm or deny this judgment and to establish reasonable weight limits for the experiments and communications equipment of the orbiter.

ACKNOWLEDGMENT

Many valuable suggestions concerning the operational capabilities of the exotic low-thrust system studied in this report were offered by W. C. Isley of the Advanced Missions and Research Section.

Goddard Space Flight Center
National Aeronautics and Space Administration
Greenbelt, Maryland, September 21, 1966
188-48-01-05-51

REFERENCES

1. Hughes, J. V., and Nomicos, G. N., "One-way Reconnaissance to Mars," in: *Advances in the Aeronautical Sciences: Proceedings of the 6th Annual Meeting of the American Astronautical Society,* 6, New York, N. Y.: MacMillan Company, January 18-21, 1961, pp. 744-759.

2. Stambler, I., "Interplanetary Probes," *Space/Aeronautics* 42(1):36-44, July 1964.

3. Lawden, D. F., "Entry into Circular Orbits," *J. Brit. Interplanetary Soc.* 13(1):27-32, January 1954.

4. Ehricke, K. A., *Space Flight,* Vol. II. "Dynamics," Princeton, New Jersey: D. Van Nostrand Company, Inc., 1962.

5. Duck, K., "An Approximation Method for Determination of Propulsion Requirements Associated with Low Thrust Orbital Transfer in a Central Force Field Under Negligible External Perturbations," GSFC Document X-623-63-117, June 1963.

6. Jensen, J., Townsend, G., "Space Flight Handbooks: Vol. 1 Orbital Flight Handbook. Part 1: Basic Techniques and Data," NASA SP 33, Part 1, N63-21101, 1963.

7. Berman, I., *The Physical Principles of Astronautics,* New York, N. Y.: John Wiley & Sons, 1961.

8. Whipple, F., *Earth, Moon, and Planets,* Cambridge, Mass.: Harvard University Press, 1963.

9. Young, V. J., "Prospects of Stereo TV from Mars Orbiter," *Space/Aeronautics* 42(5):66-68, October 1964.

10. "The National Launch Vehicle Summary," Aeronautics and Astronautics Coordinating Board of DOD-NASA, January 1964.

11. "Initial Project Development Plan — Advanced Syncom," Vol. 1 Tech. Plan, SSD 238OR, Hughes (publ. under NASA Contract 5-2797), August 1962.

Appendix A

The Optimum Orbital Radius for a Reconnaissance Satellite of Mars

1. One-Impulse Capture

That which follows, including Figure A1, is the derivation of the optimum orbital radius for a reconnaissance satellite of Mars.

In this derivation the following assumptions are made:

1. The spacecraft is travelling on a transfer ellipse bringing it to the vicinity of Mars with a hyperbolic excess velocity of V_∞ with respect to Mars.
2. A single, high-impulse velocity increment ΔV can be effected by a high-thrust Mars injection rocket motor of the spacecraft.
3. The transfer trajectory of the spacecraft is such as to bring it to the desired altitude over Mars moving horizontally (Figure A1) without any relative energy penalty.

From energy conservation in the entry trajectory from point ① to point ② (Figure A1) we can write

$$\underbrace{\left[\frac{1}{2} V_\infty^2 - \frac{\mu_{\text{Mars}}}{r_\infty}\right]}_{\substack{\text{Total Energy} \\ \text{At ①}}} = \underbrace{\left[\frac{1}{2} V_r^2 - \frac{\mu_{\text{Mars}}}{r}\right]}_{\substack{\text{Total Energy} \\ \text{At ②}}} . \qquad \text{(A1)}$$

But from the balance of gravity and centrifugal forces, the circular velocity at radius r is given by

$$\frac{V_{c,r}^2}{r} = \frac{\mu_{\text{Mars}}}{r^2} ,$$

or

$$V_{c,r}^2 = \frac{\mu_{\text{Mars}}}{r} . \qquad \text{(A2)}$$

Substituting Equation A2 in Equation A1, and solving for V_r gives

$$V_r^2 = 2V_{c,r}^2 + V_\infty^2 . \qquad \text{(A3)}$$

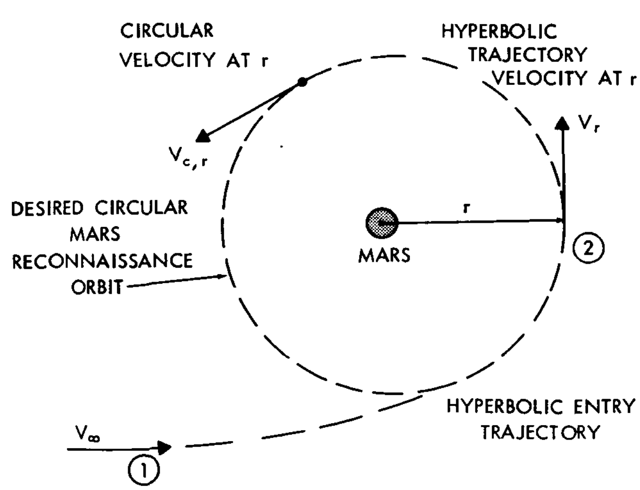

Figure A1—One-impulse Mars capture geometry.

At point ②, to achieve the circular velocity, a breaking ΔV is applied such that

$$\Delta V = V_r - V_{c,r} \quad . \tag{A4}$$

Equation A3 in Equation A4 gives

$$\Delta V = \left[V_\infty^2 + 2V_{c,r}^2\right]^{1/2} - V_{c,r} \quad . \tag{A5}$$

In Equation A5, ΔV may be minimized with respect to V_c by noting that

$$\frac{d\Delta V}{dV_{c,r}} = 2\left[V_\infty^2 + 2V_{c,r}^2\right]^{-1/2} V_{c,r} - 1 = 0 \quad ,$$

when

$$\frac{1}{2}\left[V_\infty^2 + 2V_{c,r}^2\right]^{1/2} = V_{c,r} \quad . \tag{A6}$$

Squaring both sides of Equation A6 gives

$$4V_{c,r}^2 - 2V_{c,r}^2 = V_\infty^2 \quad ,$$

or a minimax ΔV is reached when

$$2V_{c,r}^2 = V_\infty^2 \tag{A7}$$

Equation A7 in Equation A5 determines the minimax ΔV as

$$\Delta V\,(\text{minimax}) = \left[2V_{c,r}^2 + 2V_{c,r}^2\right]^{1/2} - V_{c,r} = V_{c,r} \tag{A8}$$

Equation A7 is a *minimum* ΔV condition since, from Equation A5, ΔV is always positive and, from Equation A6, only a single real-positive minimax ΔV exists. From Equations A8 and A7, $\Delta V\,(\text{minimax}) = 0.707\,V_\infty$. But from Equation A5, for $V_{c,r} = 0$; $\Delta V = V_\infty$. Thus $\Delta V = 0.707\,V_\infty$ is an *absolute minimum* velocity requirement, and the minimum one-pulse capture velocity increment is

$$\Delta V = 0.707 V_\infty \tag{A9}$$

Solving for the optimum one-impulse radius from Equations A7 and A2 shows that this occurs when

$$2V_{c,r}^2 \text{ (optimum)} = V_\infty^2 = \frac{2\mu_{Mars}}{r\text{(optimum)}} ,$$

or

$$r_m \text{ (optimum)} = \bar{r} = \frac{2\mu_{Mars}}{V_\infty^2} . \tag{A10}$$

From Reference A1

$$\mu_{Mars} = 0.0429 \times 10^6 \; \frac{km^3}{sec^2} .$$

Therefore, from Equation A10 the optimum, one-impulse Mars reconnaissance orbit radius is

$$r \text{ (optimum)} = \frac{2 \times 0.0429 \times 10^6}{(2.60)^2}$$

$$= 12{,}700 \text{ km} . \tag{A11}$$

The radius of Mars (Reference A1) is 3415 km (see Figure 4). Equation A2 in Equation A5 gives the general one-impulse capture requirement for circular orbit as

$$\Delta V = \left[V_\infty^2 + \frac{2\mu_{Mars}}{r}\right]^{1/2} - \left[\frac{\mu_{Mars}}{r}\right]^{1/2} . \tag{A11a}$$

Equation A11a, for V_∞ = 2.6 km/sec and μ_{Mars} = 0.0429×10^6 km^3/sec^2, is graphed in Figure 4.

2. Two-Impulse Terminal Maneuver

For discussion of a two-impulse terminal maneuver these assumptions are made:

1. The spacecraft is travelling on an interplanetary transfer ellipse bringing it to the vicinity of Mars with a hyperbolic excess velocity of V_∞ with respect to Mars.
2. Two velocity increments ΔV can be effected by the high-thrust Mars injection stage of the spacecraft.
3. The transfer trajectory of the spacecraft is such as to bring it to a point close to the surface of Mars moving horizontally.

4. The braking effect of the Martian atmosphere on the spacecraft during the two-impulse capture maneuver is negligible.

5. The optimum two-impulse maneuver is assumed to consist of a braking thrust at closest initial Mars approach followed by an apocenter kick from the intermediate transfer Mars-centered ellipse into the desired circular orbit (Figure A2).

The following symbols are used in Figure A2:

V_∞ ≡ hyperbolic excess velocity on entry into the vicinity of Mars from the interplanetary transfer ellipse

V_{r_m} ≡ velocity on hyperbolic entry trajectory near the surface of Mars (at r_m from the center of Mars)

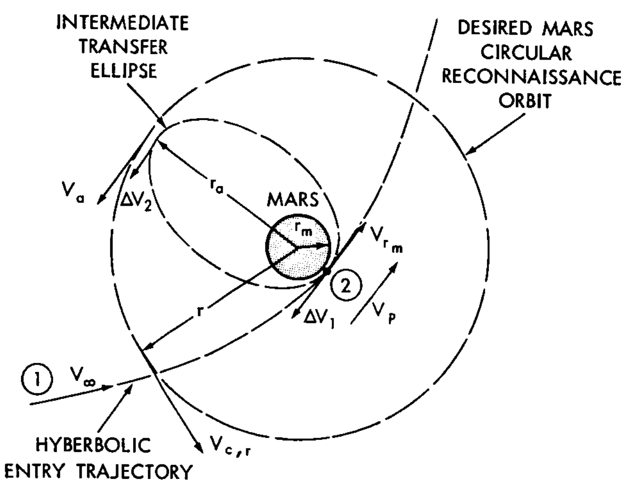

Figure A2—Two-impulse Mars capture geometry.

V_a ≡ apocenter velocity in the intermediate transfer ellipse

$V_{c,r}$ ≡ circular velocity in the desired Mars reconnaissance orbit

r ≡ radius of desired circular Mars orbit

ΔV_1 ≡ braking ΔV at r_m in the entry trajectory

ΔV_2 ≡ apocenter kick ΔV at r_a in the intermediate transfer ellipse

V_p ≡ pericenter velocity in the intermediate transfer ellipse (at r_m)

r_m ≡ distance from the center of Mars to point of nearest spacecraft approach.

Writing the energy balance in the entry trajectory between point ① and point ② (Figure A2) gives

$$\left[\frac{1}{2} V_\infty^2 + \frac{\mu_{Mars}}{r_\infty}\right]_{\substack{\text{Total Enetgy}\\ \text{At ①}}} = \left[\frac{1}{2} V_{r_m}^2 - \frac{\mu_{Mars}}{r_m}\right]_{\substack{\text{Total Energy}\\ \text{At ②}}} \tag{A12}$$

From the vis-viva integral, Equation 1, applied to the intermediate transfer ellipse

$$V_a = \left[\frac{2\mu_{Mars}}{(r_a + r_m)}\right]^{1/2} \left[\frac{(r_a + r_m)}{r_a} - 1\right]^{1/2}$$

$$= \left[\frac{2\mu_{Mars}}{r + r_m}\right]^{1/2} \left[\frac{r + r_m}{r} - 1\right]^{1/2} , \tag{A13}$$

since $r = r_a$.

Similarly,

$$V_p = \left[\frac{2\mu_{Mars}}{r + r_m}\right]^{1/2} \left[\frac{(r + r_m)}{r_m} - 1\right]^{1/2} . \tag{A14}$$

To establish the intermediate transfer ellipse, let

$$\Delta V_1 = V_{r_m} - V_p = \Delta V \text{ (eccentric capture)}$$

$$= \left[V_\infty^2 + \frac{2\mu_{Mars}}{r_m}\right]^{1/2} - \left\{\frac{2\mu_{Mars}}{r + r_m}\left[\frac{r + r_m}{r_m} - 1\right]\right\}^{1/2} , \tag{A15}$$

(from Equations A12 and A14). Equation A15, it is noted, is just the total retro-ΔV required to effect capture into an eccentric Mars orbit of periapsis r_m and apoapsis r, from a hyperbolic excess of V_∞.

To establish the desired circular reconnaissance orbit let

$$\Delta V_2 = V_{c,r} - V_a$$

$$= \left[\frac{\mu_{Mars}}{r}\right]^{1/2} - \left\{\frac{2\mu_{Mars}}{r + r_m}\left[\frac{r + r_m}{r} - 1\right]\right\}^{1/2} , \tag{A16}$$

(from Equations A2 and A13). Thus the total required velocity increment in the two-impulse terminal maneuver is (from Equations A15 and A16)

$$\Delta V = \Delta V_1 + \Delta V_2 = \left[V_\infty^2 + \frac{2\mu_{Mars}}{r_m}\right]^{1/2} - \left\{\frac{2\mu_{Mars}}{r + r_m}\left[\frac{r + r_m}{r_m} - 1\right]\right\}^{1/2}$$

$$- \left\{\frac{2\mu_{Mars}}{r + r_m}\left[\frac{r + r_m}{r} - 1\right]\right\}^{1/2} + \left[\frac{\mu_{Mars}}{r}\right]^{1/2} . \tag{A17}$$

Equation A17 can be rewritten as

$$\Delta V = \left[V_\infty^2 + \frac{2\mu_{Mars}}{r_m}\right]^{1/2} - \left(2\mu_{Mars}\right)^{1/2}\left\{\left[\frac{1}{r_m} - \frac{1}{r + r_m}\right]^{1/2} + \left[\frac{1}{r} - \frac{1}{r + r_m}\right]^{1/2}\right\} + \left[\frac{\mu_{Mars}}{r}\right]^{1/2}$$

$$= \left[V_\infty^2 + \frac{2\mu_{Mars}}{r_m}\right]^{1/2} - \left(2\mu_{Mars}\right)^{1/2}\left\{\left[\frac{r}{r_m(r + r_m)}\right]^{1/2} + \left[\frac{r_m}{r(r + r_m)}\right]^{1/2}\right\} + \left[\frac{\mu_{Mars}}{r}\right]^{1/2}$$

$$= \left[V_\infty^2 + \frac{2\mu_{Mars}}{r_m}\right]^{1/2} - \left(2\mu_{Mars}\right)^{1/2}\left\{\frac{1}{(r + r_m)^{1/2}}\left[\left(\frac{r}{r_m}\right)^{1/2} + \left(\frac{r_m}{r}\right)^{1/2}\right]\right\} + \left[\frac{\mu_{Mars}}{r}\right]^{1/2}$$

$$= \left(\frac{2\mu_{Mars}}{r_m}\right)^{1/2}\left\{\left[\frac{V_\infty^2}{\left(\frac{2\mu_{Mars}}{r_m}\right)} + 1\right]^{1/2} - \left[\frac{1}{\left(\frac{r}{r_m}\right) + 1}\right]^{1/2}\left[\left(\frac{r}{r_m}\right)^{1/2} + \left(\frac{r}{r_m}\right)^{-1/2}\right] + \frac{1}{\sqrt{2}}\left[\frac{r}{r_m}\right]^{-1/2}\right\} . \tag{A18}$$

Optimizing ΔV from Equation A18 with respect to the dimensionless ratio r/r_m, which fixes the desired reconnaissance orbit (r) for a given close approach to Mars (r_m), gives

$$\left.\frac{d\Delta V}{d\left(\frac{r}{r_m}\right)}\right|_{(r/r_m)_{optimum}} = \left(\frac{2\mu_{Mars}}{r_m}\right)^{1/2}\left\{-\frac{1}{2}\left[\frac{1}{\left(\frac{r}{r_m}\right)+1}\right]^{-1/2}\left[\left(\frac{r}{r_m}\right)^{1/2}+\left(\frac{r}{r_m}\right)^{-1/2}\right]-\left[\frac{1}{\left(\frac{r}{r_m}+1\right)^2}\right]\right.$$

$$\left.-\left[\frac{1}{\frac{r}{r_m}+1}\right]^{1/2}\left[\frac{1}{2}\left(\frac{r}{r_m}\right)^{-1/2}-\frac{1}{2}\left(\frac{r}{r_m}\right)^{-3/2}\right]-\frac{1}{2\sqrt{2}}\left(\frac{r}{r_m}\right)^{-3/2}\right\} = 0 \; . \qquad \text{(A19)}$$

When Equation A19 is simplified, (r/r_m) optimum satisfies

$$\frac{-1}{\left[\left(\frac{r}{r_m}\right)+1\right]^2}\left[\frac{\frac{r}{r_m}+1}{\left(\frac{r}{r_m}\right)}\right]^{1/2}\left[\frac{r}{r_m}+1\right]+\frac{\left[\left(\frac{r}{r_m}\right)^{3/2}-\left(\frac{r}{r_m}\right)^{1/2}\right]}{\left(\frac{r}{r_m}\right)^2\left[\frac{r}{r_m}+1\right]^{1/2}} = \frac{-\left(\frac{r}{r_m}\right)^{-3/2}}{\sqrt{2}} \; ,$$

$$\frac{-\left(\frac{r}{r_m}\right)\left[\left(\frac{r}{r_m}\right)+1\right]^{1/2}\left[\left(\frac{r}{r_m}\right)+1\right]}{\left[\left(\frac{r}{r_m}\right)+1\right]^2}+\frac{\left(\frac{r}{r_m}\right)^3-\left(\frac{r}{r_m}\right)^2}{\left(\frac{r}{r_m}\right)^2\left[\left(\frac{r}{r_m}\right)+1\right]^{1/2}} = \frac{-1}{\sqrt{2}} \; ,$$

$$\frac{-\left(\frac{r}{r_m}\right)}{\left[\left(\frac{r}{r_m}\right)+1\right]^{1/2}}+\frac{\frac{r}{r_m}-1}{\left(\frac{r}{r_m}+1\right)^{1/2}} = -\frac{1}{\sqrt{2}} \; ,$$

$$\frac{-1}{\left[\left(\frac{r}{r_m}\right)+1\right]^{1/2}} = \frac{-1}{\sqrt{2}} \; ,$$

$$\frac{r}{r_m}+1 = 2 \; ,$$

or

$$\left(\frac{r}{r_m}\right)_{optimum} = 1 \qquad \text{(A20)}$$

Actually the minimax (r/r_m) from Equation A20 is a point of relative *and* absolute maximum for the total ΔV, as can be seen by plotting ΔV vs (r/r_m) from Equation A18 for $(r/r_m) \geq 1$ (Figure 4). In this range of r/r_m, ΔV is a monotonically *decreasing* function of (r/r_m) for all r_m and $V_\infty > 0$. From Equation A18 the absolute minimum ΔV for the two-impulse capture is attained for achieving a circular orbit at infinity $(r/r_m \to \infty)$ where

$$\Delta V_{\substack{\text{two-impulse}\\ \text{minimum}\\ (r/r_m\to\infty)}} = \left(\frac{2\mu_{Mars}}{r_m}\right)^{1/2}\left\{\left[\frac{V_\infty^2}{\left(\frac{2\mu_{Mars}}{r_m}\right)}+1\right]^{1/2}-1\right\} \; . \qquad \text{(A21)}$$

It may be shown from L'Hopital's rule that the ΔV two-impulse minimum goes to zero as r_m, the closest Mars approach in the capture at infinity maneuver, goes to zero.

3. *Comparison of One- and Two-Impulse Captures*

Figure 4 shows two typical two-impulse capture velocity requirement curves for minimum Mars approaches of 0 and 1000 km altitudes. These curves suggest that for Mars capture into circular orbits with a radius below the optimum one-impulse orbit ($\bar{r}$ = 12,700 km), the one-impulse maneuver has less velocity requirement. Conversely, for capture into orbits greater than the optimum one-impulse orbit, the two-impulse maneuver has less velocity requirement.

That a crossover point between the two types of capture maneuver exists for minimum Mars encounters at less than one-impulse optimum is evident from the general nature of the two velocity functions as previously discussed and illustrated in Figure 4. To show that the optimum one-impulse orbit solution is the general crossover solution for all two-impulse captures into orbits from a minimum Mars encounter distance less than one-impulse optimum, it is only necessary to show that the one-impulse optimum solution is also a general two-impulse capture solution.

The one-impulse optimum capture solution is (from Equations A10 and A9)

$$\Delta V = 0.707 V_\infty \tag{A22}$$

at,

$$r = \bar{r} = \frac{2\mu_{Mars}}{V_\infty^2} . \tag{A23}$$

Equation A23 divided by r_m gives

$$\frac{r}{r_m} = \frac{2\mu_{Mars}}{V_\infty^2 r_m} . \tag{A24}$$

For a two-impulse capture into an $r = \bar{r}$ orbit Equation A24 in Equation A18 will give

$$\Delta V = V_\infty \left\{ \left[1 + \frac{\bar{r}}{r_m}\right]^{1/2} - \left[\frac{1}{\frac{\bar{r}}{r_m} + 1}\right]^{1/2} \left[\frac{\bar{r}}{r_m} + 1\right] + \frac{1}{\sqrt{2}} \right\}$$

$$= \frac{V_\infty}{\sqrt{2}} = 0.707 V_\infty , \tag{A25}$$

which is the optimum one-impulse velocity requirement.

To summarize then, between the two types of maneuvers discussed:

1. For circular Mars orbiters less than 12,700 km from the center of Mars, one-impulse captures are optimum.

2. For circular Mars orbiters greater than 12,700 km from the center of Mars, two-impulse captures are optimum.

REFERENCES

A1. Jensen, J., Townsend, G., "Space Flight Handbooks: Vol. 1 Orbital Flight Handbook. Part 1: Basic Techniques and Data," NASA Pub. SP-33, Part 1, N63-21101, 1963.

Appendix B

Derivation of the Fundamental Free Space, Constant Thrust Rocket Equations

Consider a rocket of mass m_0 initially at rest with respect to a coordinate system whose origin is located at the center of mass of the system at time t_0 (Figure B1a). It suddenly expels an exhaust propellant particle of mass Δm_p in the $-x$ direction at a velocity C with respect to the center of mass. At the time $t = t_0 + \Delta t$, the rocket body now has a mass $m = m_0 - \Delta m_p$ moving with a velocity ΔV in the $+x$ direction (Figure B1b). From the conservation of momentum, the center of mass of the system, which is composed of Δm_p and m, will be at the same position at time t as it was at time t_0, since no external forces act on this total mass system.

From Figure B1b, then, the invariance of the "rest" center of mass means that

$$m\Delta V = \Delta m_p C . \tag{B1}$$

The left side of Equation B1 is the momentum gain of the rocket mass m during the very short time interval Δt of the action. By the first integral of Newton's second law (impulse-momentum) this implies that an effective thrust T_e has been acting on the rocket body m over t such that

$$m\Delta V = T_e \Delta t . \tag{B2}$$

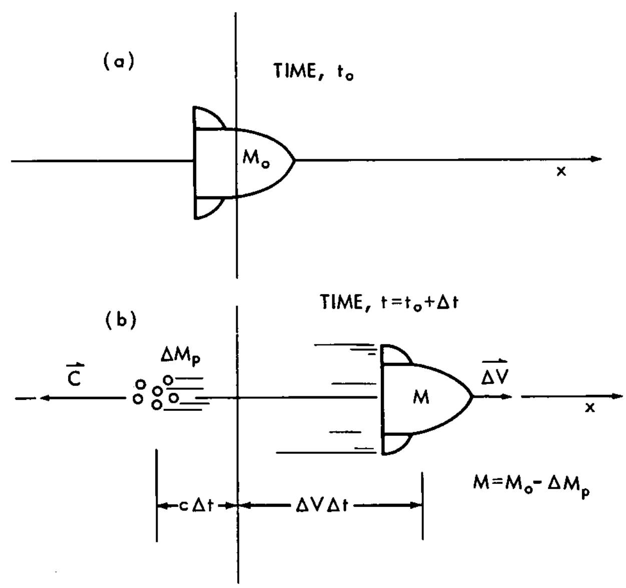

Figure B1—(a) Initial time (t_0) configuration of rocket; (b) configuration of rocket at $t_0 + \Delta t$.

From Equation B1 and B2 then

$$\Delta m_p C = T_e \Delta t , \tag{B3}$$

or,

$$T_e = \frac{C\Delta m_p}{\Delta t} , \tag{B4}$$

which is the effective thrust on the free space rocket. Also from Equation B3 it is seen that

$$C = \frac{T_e \Delta t}{\Delta m_p} = gI_{sp} , \tag{B5}$$

since from its definition, I_{sp} is the total impulse on a rocket per unit weight of fuel expelled. Equation B5 in Equation B1 gives

$$m\Delta V = gI_{sp} \Delta m_p . \tag{B6}$$

If Δm is the incremental change in the rocket mass during the action time Δt, then clearly

$$\Delta m = -\Delta m_p ,$$

or from Equation B6

$$m\Delta V = -gI_{sp} \Delta m . \tag{B6a}$$

It is irrelevant to the argument leading to Equation B6a whether m_0 is initially at rest or moving with a velocity V if C is interpreted as the free space exhaust velocity with respect to the rocket body at t_0 when the propellant is expelled. During the action time of Δm_p expulsion, Δt, the center of mass position of m at t_0 continues to translate at a constant velocity V from Newton's first law. Figures B1 and B2 are then to be pictured in a coordinate system moving at V with respect to the x-axis and ΔV is then interpreted as a change in the velocity V of the rocket at time t_0.

Equation B6a may thus be rewritten as a differential equation expressing the rocket action at any time when the mass of the rocket is m and its velocity is V

$$dV = gI_{sp} \frac{dm}{m} . \tag{B7}$$

Integrating Equation B7 gives the velocity at any time,

$$V = -gI_{sp} \ln m + K.$$

If $V = V_0$ when $m = m_0$, then

$$K = V_0 + gI_{sp} \ln m .$$

Thus the total incremental velocity of the rocket as the mass changes from m_0 to m is

$$\Delta V = V - V_0 = gI_{sp} \left\{ -\ln m + \ln m_0 \right\} ;$$

or

$$\Delta V(\text{of rocket}) = gI_{sp} \ln \frac{m_0}{m} ,$$

and the mass of the rocket after the ΔV increment is

$$m = m_0 \, e^{-\Delta v / gI_{sp}} ,$$

or in terms of the weight of the rocket,

$$W = W_0 \, e^{-\Delta v / gI_{sp}} . \tag{B8}$$

To determine the time necessary for the rocket to achieve $\Delta V(\text{total}) = V - V_0$, note that the mass of the rocket at any time is given by

$$m = m_0 - \dot{m} t , \tag{B9}$$

where

$$\dot{m} = \frac{\Delta m}{\Delta t} = \frac{dm}{dt}$$

for a continuous expulsion of mass. But from Equations B4 and B5

$$T_e = gI_{sp} \, \dot{m} . \tag{B10}$$

Equation B10 in Equation B9 gives

$$m - m_0 = \frac{-T_e \, t}{gI_{sp}} . \tag{B11}$$

From Equation B8, Equation B11 becomes

$$t = -gI_{sp}\left(m - m_0\right) = \frac{-gI_{sp}\, m_0}{T_e}\left\{e^{-\Delta v/gI_{sp}} - 1\right\}$$

$$= \frac{W_0\, I_{sp}}{T_e}\left\{1 - e^{-\Delta v/gI_{sp}}\right\} . \qquad \text{(B12)}$$

Because of its occurrence in the free space, constant thrust rocket Equations B8 and B12, it is convenient to define a characteristic mission parameter, M, associated with a total mission Δv made up by a rocket engine of specific impulse I_{sp} as

$$M = e^{-\Delta v/gI_{sp}} \qquad \text{(B13)}$$

(Figure 1). Then the rocket weight loss and mission (or engine "on") time equations, Equations B8 and B12, for a rocket in free space become

$$W = W_0\, M , \qquad \text{(B14)}$$

and

$$t = \frac{W_0 I_{sp}}{T_e}(1 - M) . \qquad \text{(B15)}$$

Appendix C

Orbit Transfer by Low, Continuous Circumferential Thrusting vs the Hohmann Semiellipse

The velocity requirement for low, continuous circumferential-thrusting, circular coplanar orbit transfer, is established in Reference C1 as

$$\Delta V(\text{continuous})_{r_1 \to r_2,\ r_1 < r_2} = \left(\frac{\mu}{r_1}\right)^{1/2} - \left(\frac{\mu}{r_2}\right)^{1/2} , \tag{C1}$$

providing the thrust to mass ratio is sufficiently less than the local gravitational acceleration. In a Hohmann cotangential semiellipse, (Figure C1, for example) establishing the minimum two-impulse transfer trajectory between coplanar circular orbits r_1 and r_2 $(r_1 < r_2)$ of a planet whose gravitational constant is μ, the pericenter velocity is (from Equation A14)

$$V_p = \left(\frac{2\mu}{r_1 + r_2}\right)^{1/2} \left[\frac{r_1 + r_2}{r_1} - 1\right]^{1/2} . \tag{C2}$$

The apocenter velocity is (from Equation A13)

$$V_a = \left(\frac{2\mu}{r_1 + r_2}\right)^{1/2} \left[\frac{r_1 + r_2}{r_1} - 1\right]^{1/2} . \tag{C3}$$

The circular velocities at r_1 and r_2 are

$$V_{c,r_1} = \left(\frac{\mu}{r_1}\right)^{1/2} \tag{C4a}$$

and

$$V_{c,r_2} = \left(\frac{\mu}{r_2}\right)^{1/2} . \tag{C4b}$$

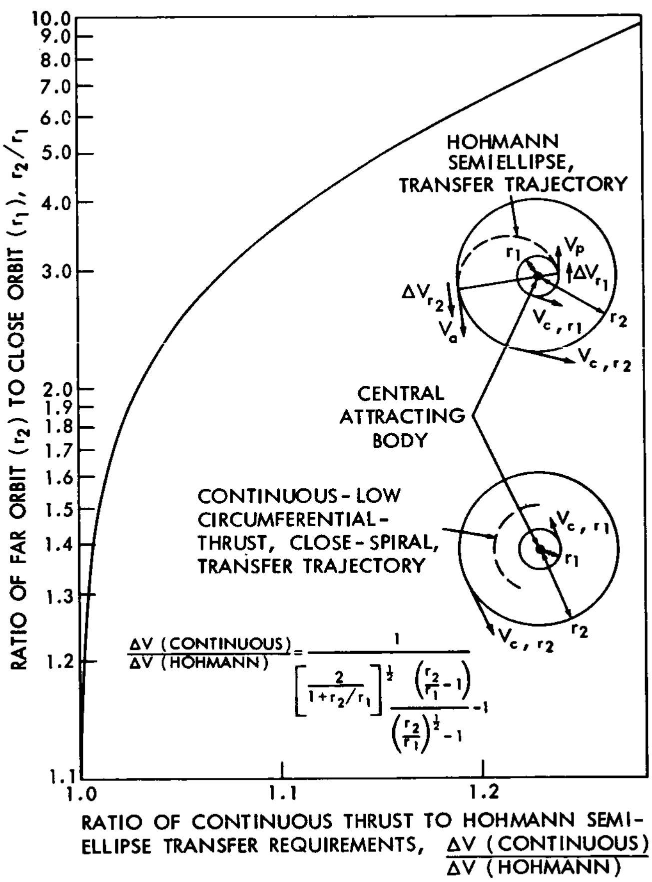

Figure C1—Continuous, low circumferential thrust vs. Hohmann semiellipse requirements for orbit transfer.

The velocity requirement to enter the Hohmann semiellipse at r_1 for transfer $r_1 \to r_2$ is Equation C2 minus Equation C4a, or

$$\Delta V_{r_1} (\text{Hohmann}) = \left(\frac{2\mu}{r_1 + r_2}\right)^{1/2} \left[\frac{r_1 + r_2}{r_1} - 1\right]^{1/2} - \left(\frac{\mu}{r_1}\right)^{1/2} \tag{C5}$$

The velocity requirement to leave the Hohmann semiellipse at r_2, for transfer $r_1 \to r_2$, is Equation C4b minus Equation C3, or

$$\Delta V_{r_2} (\text{Hohmann}) = \left(\frac{\mu}{r_2}\right)^{1/2} - \left(\frac{2\mu}{r_1 + r_2}\right)^{1/2} \left[\frac{r_1 + r_2}{r_2} - 1\right]^{1/2} \tag{C6}$$

The total Hohmann transfer requirement is Equation C6 plus Equation C5 or

$$\underset{r_1 \to r_2,\ r_1 < r_2}{\Delta V(\text{Hohmann})} = \left(\frac{\mu}{r_2}\right)^{1/2} - \left(\frac{\mu}{r_1}\right)^{1/2} + \left(\frac{2\mu}{r_1 + r_2}\right)^{1/2} \left[\left(\frac{r_2}{r_1}\right)^{1/2} - \left(\frac{r_1}{r_2}\right)^{1/2}\right]^{1/2} \tag{C7}$$

Equation C7 divided by Equation C1 gives the ratio of continuous thrust to Hohmann semiellipse transfer requirements as

$$\frac{\Delta V(\text{continuous})}{\Delta V(\text{Hohmann})} = \frac{1}{\left[\frac{2}{1 + (r_2/r_1)}\right]^{1/2} \frac{\left[(r_2/r_1) - 1\right]}{(r_2/r_1)^{1/2} - 1} - 1} \tag{C8}$$

(see Figure C1). Equation C8 also gives the transfer comparison for changing from far orbits r_2 to close orbits r_1, as the maneuvers in both continuous and Hohmann cases are merely reversed in thrust direction, the energy requirements remaining the same.

REFERENCES

C1. Duck, K., "An Approximation Method for Determination of Propulsion Requirements Associated with Low Thrust Orbital Transfer in a Central Force Field Under Negligible External Perturbations," GSFC Document X-623-63-117, June 1963.

Appendix D

An Off-the-Shelf Spacecraft for a Mars Orbiter Mission with an Atlas/Centaur or Titan II/Agena D Boost (for Launch Dates in 1966)

In considering the Mars orbiter spacecraft, the payload in orbit will be broken down into six subsystem categories: (A) stability and attitude control, (B) Mars-geophysical experiments (including structural and electronic integration), (C) TV cameras and accessories; (D) spacecraft support structure (including thermal control), (E) power supply, and (F) communications and associated electronics.

Flight subsystem weights from the EGO (Eccentric (orbiting) Geophysical Observatory), Mariner, and Nimbus spacecrafts are chosen as appropriate, with various scale factors, to make up the Mars orbiter subsystems above. Table D1 below gives the actual weight breakdowns for the EGO, Mariner and Nimbus spacecraft.

As a target, a spacecraft including the Nimbus APT (automatic picture transmission) TV camera system (with two cameras) and 33 percent of the EGO geophysical experiments package, will be aimed for. The target Mars orbit will be the eccentric synchronous one (pericenter altitude, 1000 km). The payload target is 815 pounds (see Table 1).

We now put together a typical 1966 Mars orbiter spacecraft from the components of the spacecraft of Table D1. The following spacecraft system percentages are assigned as the basis for the weight scaling to make up a first try at an 815 pound spacecraft built around 33 percent of the EGO package and the Nimbus medium-resolution TV system:

(A) *Stability and Attitude Control:* Use 100 percent of the EGO subsystem scaled to 815 pounds (for the Mars orbit phase of the mission) plus 50 percent of the Mariner subsystem scaled to 1250 pounds (for the Mars transfer and injection phases of the mission). The attitude restraints for the information-gathering phase of the Mars orbiter mission should be less severe than in the EGO mission, as the eccentricity of the Mars orbit is less. On the other hand, attitude restraints for the data transmission phase will be more severe because of the need for higher antenna gain and consequent greater pointing accuracy over the greater distance of the Earth-Mars link. There is need for additional attitude control in the Mars transfer and Mars injection phases. A weight allotment for this function of 50 percent of the Mariner subsystem scaled to 1250 pounds (the spacecraft weight in the Mars transfer trajectory) is considered sufficient, since the task will actually be performed by the basic scaled-EGO subsystem with an increase only in tankage and propellant weight.

Table D1

Flight Subsystem Weights (pounds) for a Mars Orbiter Type Spacecraft.

Subsystem	Spacecraft			"Off-the-Shelf" Proposed Reconnaissance Mars Orbiter for 1966 Launch Dates†
	Mariner*	EGO**	Nimbus**	
A. Stability and Altitude Control	59	135	135	185
B. Geophysical Experiments	41	366	133 includes high resolution TV system	105
C. TV Cameras and Accessories (including electronics)			22 one camera, low resolution	44 two cameras, low resolution
D. Structure	100	204	231	167
E. Power Supply	108	200	204	202
F. Communications and Associated Electronics	110	146	107	110
G. Trajectory Propulsion (already accounted for by booster for Mars orbiter mission)	36			
Contingency	6			
Total S/C Weight	460	1051	812	813†

*From Space Programs Summary no. 37-12, Vol. 1, JPL, 1 December 1961.

**Private communication from M. L. Moseson, NASA-GSFC, November 1964.

†This does not include dead Mars stage engine, which is assumed to be separated in Mars orbit. With dead Mars stage in orbit, the spacecraft weight is about 880 lb.

Mars Orbit Specifications:

pericenter altitude	1000 km
apocenter altitude	33,000 km
period	about 24 hrs
booster	Titan II/Agena-D or Atlas/Centaur
Mars stage	JPL solid, with "ATS" apogee motor performance.

(B) *Geophysical-Type Experiments:* As a first trial 33 percent of the EGO subsystem will be used. The particular experiments carried can begin with a base having the minimum experiments of the Mariner spacecraft (40 pounds) — infrared and microwave scanning sensors and simple magnetometers and electron-proton particle counters. The eccentric Mars orbiter should offer an excellent vertical sampling of the radiation and upper atmosphere molecular environment around Mars.

(C) *TV Cameras and Accessories* (medium resolution): The requirement will be 200 percent of the Nimbus APT subsystem (44 pounds for two cameras).

(D) *Structure:* Here the requirement is 50 percent of the Mariner subsystem plus 50 percent of the EGO subsystem scaled to 815 pounds. The division is arbitrary. The spacecraft structure fractions (of the in-orbit weight) in either case are close to 0.20.

(E) *Power Supply:* The power supply weight will be 78 percent of the weight of the experiment package, the TV subsystem and the communications and electronics subsystem. The Mariner power supply weight-to-affected subsystems weight fraction is 0.72, with the chief consideration beging long distance communication. The equivalent fraction for the Nimbus spacecraft is 0.84, with the chief consideration being the heavy power-energy demands of the TV subsystems. The equivalent EGO power supply fraction, where neither of these considerations apply, is only 0.39.

(F) *Communications and Associated Electronics:* These are 100 percent of the Mariner subsystem. The Mariner subsystem as a whole is considered sufficient to handle the long distance communications load of the Mars orbiter, which includes a tracking transponder.

The actual calculation of the first trial 815 pound Mars orbiter subsystem weights on the above basis is as follows:

(A) *Stability and Attitude Control*

$$\text{weight} = \frac{135(\text{EGO}) \times 815}{1051(\text{EGO})} + \frac{0.50 \times 59(\text{Mariner}) \times 1250}{460(\text{Mariner})}$$

$$= 105 + 80 = 185 \text{ pounds.}$$

(B) *Geophysical Type Experiments* (Radiometers, magnetometers, particle counters etc.)

$$\text{weight} = 0.33 \times 366(\text{EGO}) = 120 \text{ pounds.}$$

(C) *TV Cameras* (medium resolution) *and Accessories* (includes two cameras of the Nimbus medium resolution type).

$$\text{weight} = 44 \text{ pounds.}$$

(D) *Structure*

$$\text{weight} = \frac{0.50 \times 100(\text{Mariner}) \times 815}{460(\text{Mariner})} + \frac{0.50 \times 204(\text{EGO}) \times 815}{1051(\text{EGO})}$$

$$= 88 + 79 = 167 \text{ pounds.}$$

(E) *Power Supply* (see sections B and C above and F below)

$$\text{weight} = 0.78 \times (120 + 44 + 110) = 214 \text{ pounds.}$$

(F) *Communications and Associated Electronics*

$$\text{weight} = 110 \text{ pounds (Mariner).}$$

The total first trial Mars orbiter spacecraft weight is the sum of A through F above, or

$$\text{spacecraft weight (first trial)} = 840 \text{ pounds.}$$

As a second trail, assume that only 105 pounds of EGO geophysical experiments (28.7 percent EGO) are carried by the Mars orbiter spacecraft. The subsystem B will lose 15 pounds and subsystem E will lose $0.78 \times 15 = 12$ pounds, so that the total spacecraft weight will be $840-27 = 813$ pounds.

In summary, it would appear that an unmanned Mars reconnaissance orbiter carrying about 30 percent of the geophysical sensor package of the EGO earth satellite, as well as two medium resolution TV cameras, is a practical prospect as soon as the Atlas/Centaur or Titan II/Agena D boosters become available.

It is noted however, that the weight calculations in this section are based on a total Mars orbiter spacecraft weight (including structure) of 815 pounds, which does not include the empty weight of the Mars stage rocket engine. If it is impractical to separate the dead Mars stage engine in Mars orbit, then the basic Mars orbiter spacecraft weight of 815 pounds will be increased to about 880 pounds. As a consequence, the weight of the stability and attitude control subsystems will be somewhat heavier due to the added load. The increased weight from this source would be about 135 (EGO) $\times$ (880-815)/1051 (EGO) = 8 pounds. But not all of this penalty would have to be absorbed in the experiment package, as a smaller experiment package implies a lighter power supply for the Mars spacecraft. Thus, even if the Mars stage cannot be separated, the total experiment package of about 150 pounds will not be significantly compromised (Table D1).

Appendix E

Plane Change Considerations for Mars Orbiter Missions

It was pointed out in the Preface and Discussion of this report that only gross, nominal, trajectory requirements have been taken into consideration in the calculation of payload weights for Mars missions in section II. It was also pointed out in the discussion and may be reemphasized that the method of "patched conics" used to derive these ΔV requirements is, in general, a conservative method. In one aspect, it neglects the perturbing influence of the sun and the moon, the latter body, with careful earth-escape guidance, being capable of providing some small trajectory assist in the near-earth phase of the mission (Reference E1). More important though, we have assumed a conservative Mars solar orbit, always circular at its mean distance from the sun. The actual orbit of Mars is considerably more eccentric than the orbit of the earth.

We might presume that by careful selection of the launch date, the actual hyperbolic excesses at Mars encounter will be somewhat less than that calculated in section II on the basis of the simple Hohmann semiellipse transfer between coplanar, circular earth and Mars orbits. However, a factor which we have also ignored and which must increase the requirements is the necessity of accounting for the small $\sim 1.85°$ inclination (Reference E2) of the Mars solar orbit plane with the ecliptic. In the lowest energy cases, the ecliptic plane will be close to the plane of the earth-Mars transfer orbit of the spacecraft.

There are two aspects of this "plane change" consideration for the Mars orbiter mission. One is in the earth-escape phase and one at Mars encounter. Let us first discuss the latter because, even after assuring a low-energy Mars encounter by proper injection into the Mars-transfer trajectory, a plane misalignment of $\sim 1.85°$ may still be present at that encounter. At such a Mars encounter the inertial velocity vector diagram between planet and spacecraft is shown in Figure E1.

For the low-thrust missions, $V_{\infty,M}$, or the relative velocity between Mars (considered massless) and the approaching spacecraft at or near Mars encounter, must be made up almost entirely before the in-spiralling capture maneuver can commence. For the high-thrust missions, however, only a fraction of $V_{\infty,M}$ will need to be made up in the fast-capture maneuver (see section II and Appendix A), taking advantage of retrothrusting only at closest Mars approach.

In section 2 it was assumed that

$$V_{\infty,M} = V_{Mars} - V_{s/c}$$

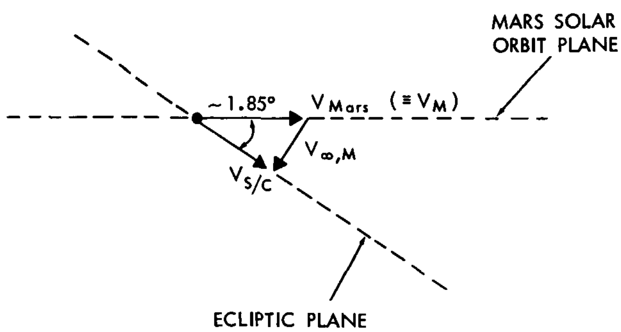

Figure E1—Inertial velocity vector orientation at Mars encounter for low-energy transfers.

or that there was no plane misalignment at Mars encounter. From Figure E1, however, we see that actually

$$V_{\infty,M} \doteq \left\{V_M^2 + V_{s/c}^2 - 2V_M V_{s/c} \cos(1.85°)\right\}^{1/2}$$

$$= \left\{V_M^2 + V_{s/c}^2 - 2V_M V_{s/c} \left[1 - \sin^2 1.85°\right]^{1/2}\right\}^{1/2} \tag{E1}$$

Since $\sin^2 1.85° << 1$, Equation E1 becomes

$$V_{\infty,M} \doteq \left\{V_M^2 + V_{s/c}^2 - 2V_M V_{s/c} + V_M V_{s/c} \sin^2 1.85°\right\}^{1/2}$$

$$= \left(V_M - V_{s/c}\right)\left\{1 + \frac{V_M V_{s/c} \sin^2 1.85°}{\left(V_M - V_{s/c}\right)^2}\right\}^{1/2} . \tag{E2}$$

But from section II, $V_M = 1.39 \times 10^{-2}$ AU/day and $V_{s/c} \doteq 1.24 \times 10^{-2}$ AU/day for the lowest energy transfers so that

$$\frac{V_M V_{s/c} \sin^2 1.85°}{\left(V_M - V_{s/c}\right)^2} = 0.0797 .$$

Thus Equation E2 becomes

$$V_{\infty,M} \doteq \left(V_M - V_{s/c}\right)(1.0398)$$

$$= 2.60 \text{ km/sec (from Section 2)} + 0.104 \text{ km/sec.} \tag{E3}$$

The added hyperbolic excess due to the plane misalignment is only 0.104 km/sec. The smallest low-thrust mission characteristic velocity from Table 2, calculated without this plane consideration, is 4.05 km/sec (for the circular synchronous Mars orbiter). The added velocity requirement due to the necessity of the plane change at Mars encounter is only about 2-1/2 percent of the total requirement and can be neglected for the purposes of these preliminary estimates.

For the favorable high-thrust Mars eccentric orbiter mission, the added velocity increment due to $\Delta V_{\infty,M} = 0.104$ km/sec can be approximated by taking the first derivative of Equation A15, the eccentric orbiter capture requirement, with respect to V_∞. This gives

$$\frac{d\left(\Delta V_{\text{eccentric capture}}\right)}{dV_{\infty,M}} = \frac{V_{\infty,M}}{\left[V_{\infty,M}^2 + \frac{2\mu_{Mars}}{r_m}\right]^{1/2}} . \tag{E4}$$

writing $\Delta(\Delta V_1) \doteq d\,\Delta V_1$ and $\Delta(V_{\infty,M}) \doteq dV_{\infty,M}$ for small finite increments of these requirements causes Equation E4 to become

$$\Delta(\Delta V_{EC}) \doteq \frac{V_{\infty,M}\,\Delta V_{\infty,M}}{\left[V_{\infty,M}^2 + \frac{2\mu_{Mars}}{r_m}\right]^{1/2}} , \qquad \text{(E5)}$$

where $V_{\infty,M}$ is the original, uncorrected hyperbolic excess (2.60 km/sec) and $\Delta V_{\infty,M} = 0.104$ km/sec. For the synchronous Mars orbiter with a minimum altitude of 1000 km,

$$\frac{2\mu_{Mars}}{r_m} = \frac{2 \times .429 \times 10^5}{(1000 + 3410)\,\text{km}}\ \text{km}^3/\text{sec}^2 = 19.4\ \text{km}^2/\text{sec}^2 .$$

Equation E5 evaluates the added requirement as

$$\Delta(\Delta V_{EC}) = \frac{2.6 \times 0.104}{[2.6^2 + 19.4]^{1/2}} = 0.0536\ \text{km/sec} . \qquad \text{(E6)}$$

Since ΔV_{EC} (from section II) is 0.95 km/sec for the synchronous eccentric orbiter, the added increment from Equation E6 is only about 5-1/2 percent of the total and can be neglected in this preliminary survey of the orbiter possibilities.

The other aspect of the plane change consideration concerns the requirement in the near-earth phase of the mission to assure an adequate Mars encounter. Theoretically, one would like to launch from earth on only those dates when the spacecraft, after about a 180°-transfer, would reach the orbit of Mars when Mars was in or near the ecliptic plane. Unfortunately, the waiting time between two such events is about 19 years. This is longer than the synodic period (about 2 years) which is the normal waiting time between any two transfers which depend on some fixed Earth-Sun-Mars configuration independent of the line of nodes between Mars and Earth solar orbits. Figure E2 illustrates the earth injection conditions which, it is conjectured, would be necessary for minimum energy Mars transfers with low hyperbolic excesses at Mars, if Mars and Earth had circular orbits.

Preliminary scan of one-way Mars trajectories in the period (1960-1970) (References E3 and E4) indicates that such near-minimum energy conditions will occur in the late 1960's and early 1970's. However, it appears that the favorable launch period in 1966/67 must utilize transfer trajectories yielding Mars hyperbolic excess velocities no less than 40 percent higher than that assumed in this preliminary study.

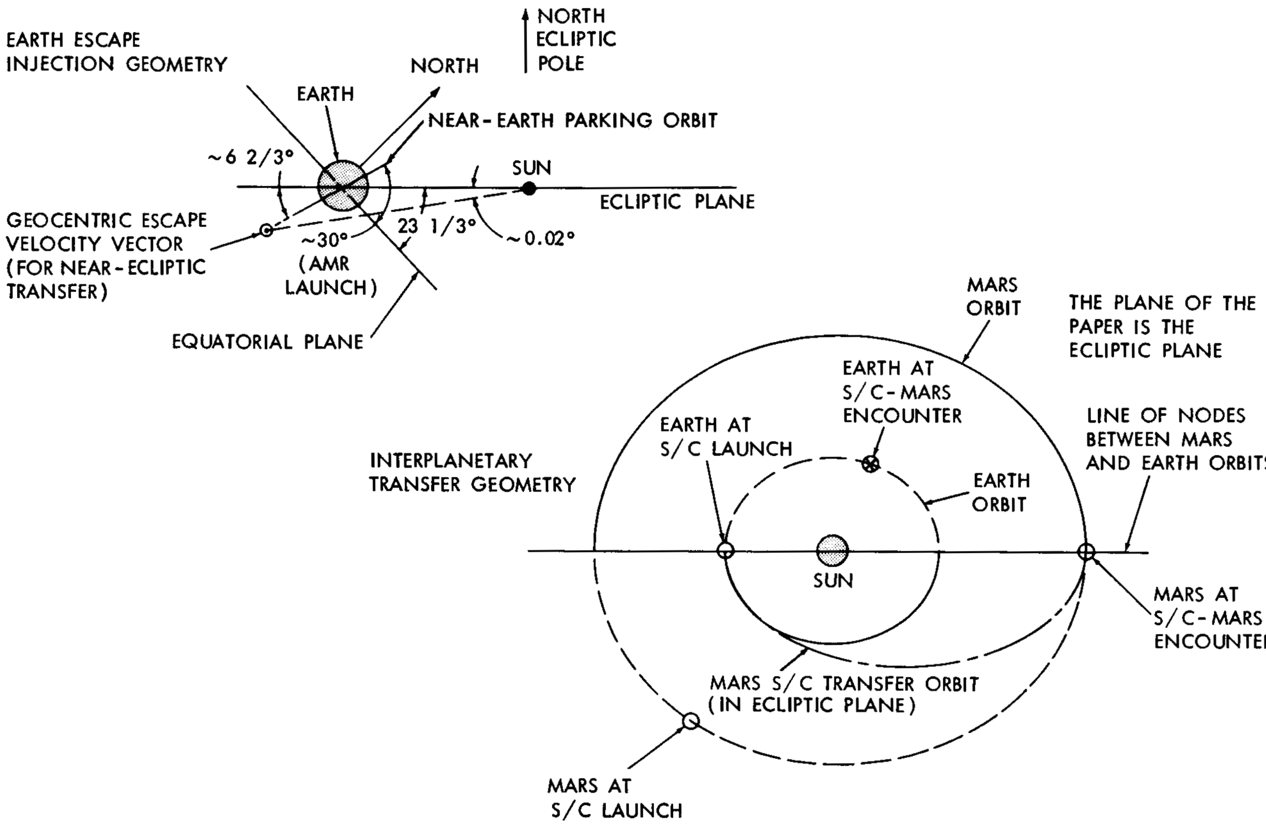

Figure E2—Earth escape injection and planetary configuration for near-minimum Mars transfer energy and hyperbolic excess velocity at Mars encounter.

REFERENCES

E1. Ehricke, K. A., *Space Flight,* Vol. II. "Dynamics," Princeton, New Jersey: D. Van Nostrand Company, Inc., 1962.

E2. Jensen, J., Townsend, G., "Space Flight Handbooks: Vol. 1 Orbital Flight Handbook. Part 1: Basic Techniques and Data." NASA SP-33, Part 1, N63-21101, 1963.

E3. Clarke, V. C., Jr., Bollman, W. E., Roth, R. Y., and Scholey, W. J., "Design Parameters for Ballistic Interplanetary Trajectories," JPL TR-32-77, N63-14717, 1963.

E4. "Space Flight Handbooks: Vol. 3, Planetary Flight Handbook," Parts 1 and 2, NASA SP-35, 1963.

Appendix F

Weight Estimates for an Optimum Low Thrust-High Thrust Mars Eccentric Orbiter Spacecraft for Launch in 1966/67

As discussed in the Introduction due to the great attractiveness of the eccentric Mars orbit, and the recent interest in low-thrust, high-performance rocket engines, we may wish to consider the mission profiles with this system which can efficiently achieve these orbits. With the guidelines of efficiency established in section III, a conceivable profile for a single Mars stage, low-thrust capture into an eccentric orbit of low Mars pericenter would be the following:

1. Escape the Earth and enter the Earth-Mars transfer ellipse via a high-thrust boost from a low earth parking orbit
2. Cancel almost all of the hyperbolic excess velocity near Mars encounter by thrusting forward for a number of days
3. Cease thrusting when the residual velocity vector with respect to Mars will bring the spacecraft to the desired minimum altitude at a velocity near that of Mars escape for this altitude
4. Retrothrust in the vicinity of pericenter to effect capture at the desired minimum altitude into an orbit just under 1.0 eccentricity
5. Continue to retrothrust at each succeeding pericenter passage until the desired apoapsis is achieved.

It is instructive to calculate the characteristic velocity for this slow eccentric capture maneuver. First of all, it will take almost all of $V_{\infty,\text{Mars}}$(2.6 km/sec) to initiate it. The true capture increment from then on is given by Equation A15 with $V_\infty = 0$. The total increment in velocity for slow capture becomes

$$\Delta V = V_{\infty,\text{Mars}} + \left(\frac{2\mu_{\text{Mars}}}{r_m}\right)^{1/2} - \left(\frac{2\mu_{\text{Mars}}}{r + r_m}\right)^{1/2}\left(\frac{r + r_m}{r_m} - 1\right)^{1/2}$$

$$= V_{\infty,\text{Mars}} + \left(\frac{2\mu_m}{r_m}\right)^{1/2}\left\{1 - \left(\frac{1}{\frac{r_m}{r} + 1}\right)^{1/2}\right\} . \tag{F1}$$

The complete capture would be effected in stages by tangential retrothrusting only in the vicinity of pericenter. For the specifications of the synchronous eccentric Mars orbiter of 1000 kilometer minimum attitude:

$$\mu_{Mars} = 0.429 \times 10^5 \ km^3/sec^2$$

$$r_m \doteq 1000 + 3400 = 4400 \ km$$

$$r \doteq 33,000 + 3400 = 36,400 \ km$$

$$r_m/r \doteq 0.121$$

$$\frac{(2\mu_{Mars})^{1/2}}{r_m} = 4.41 \ km/sec \ .$$

With these specifications, Equation F1 evaluates the total single-stage, slow-capture requirements as

$$\Delta V \ (\text{slow capture}) = 2.6 + 0.4 = 3.0 \ km/sec \ .$$

The equivalent fast-capture requirement (from Equation A15) is only 0.95 km/sec. This is because the high-thrust engine is able to brake sufficiently at once to effect capture even against a considerable hyperbolic excess in the high-speed region around pericenter where given ΔV increments effect the greatest changes in trajectory energy. Thus both $\Delta V/gI_{sp}$, which controls the mission parameter, and the engine and tankage constants will be less favorable for the single-stage, slow, low-thrust capture as against its high-thrust counterpart. The higher I_{sp} is not sufficient to counterbalance the greater ΔV of the low-thrust mission profile.

The single-stage, low-thrust parameters for this mission, employing the same engine as in section II, are

$$M_{low} = \exp\left(-\frac{3.0 \times 3281}{32.15 \times 750}\right) = 0.665 \ \text{(compared to 0.711 for the high-thrust profile)}$$

$$\dot{C}_{T\text{-}low} = 0.30$$

$$C_{E\text{-}low} = \frac{165 \ \text{pounds}}{W_0} \ \text{(for four 1/4-pounds thrust units).}$$

For earth-Mars transfer payloads of

350 - 500 pounds (Atlas Agena D) ,

1000 - 1250 pounds (Atlas Centaur or Titan II/Agena D) ,

3000 - 3500 pounds (Titan III-C) ,

'the respective engine constants are (Table 3)

$$C_{E\text{-}low}\ (\text{Atlas Agena D boost}) = 0.471 - 0.330$$

$$C_{E\text{-}low}\ (\text{Center boost}) = 0.165 - 0.132$$

$$C_{E\text{-}low}\ (\text{Titan III-C boost}) = 0.055 - 0.047\ .$$

Thus, from Equation 17, the payload fractions for the single-stage, low-thrust eccentric Mars captures are

$$(PL)_{F,Atlas} = 0.094 - 0.235\ ,$$

$$(PL)_{F,Centaur} = 0.400 - 0.433\ ,$$

$$(PL)_{F,Titan\ 3C} = 0.510 - 0.518\ .$$

The comparable payloads deliverable to this Mars eccentric orbit by a single, low-thrust upper stage are from Table 1

$$W_{PL,\ Atlas\ boost} = 33 - 118\ \text{pounds}\ ,$$

$$W_{PL,\ Centaur\ boost} = 400 - 541\ \text{pounds}\ ,$$

$$W_{PL,\ Titan\ 3C\ boost} = 1530 - 1812\ \text{pounds}\ .$$

Once again we have the general result that the higher mission energies required by the time limited capabilities of the low-thrust profiles are not counterbalanced by higher performance in the "poodle system". In addition, the greater engine and tankage weights of the low-thrust system considered appear to penalize these single-stage, high-performance systems prohibitively for all but the heavier Mars spacecraft. These general conclusions are also expected to hold true when realistic trajectory plane change requirements are taken into account. However, it may be anticipated that the low thrust-high performance system will make significant relative gains over high-thrust performance when plane change requirements are particularly severe (see Appendix E and Conclusions). These occurrences will depend on launch date for the orbiter mission.

Since the energy requirements for the single-stage, low-thrust eccentric Mars orbiter are, comparatively, too severe at the Mars end, we may wish to consider a two-stage operation: low-thrust in earth orbit, high-thrust for Mars capture.

In general, any additional staging reduces the reliability of a mission. However, in this case there are compensating factors. The separation operation will be performed in earth orbit where the liklihood of its success will be greater than if a comparative staging operation were performed in Mars orbit. A typical mission profile might be as follows:

1. Boost a heavy spacecraft into a low earth-parking orbit;

2. Use low thrust-high performance boost to raise the spacecraft to an optimum altitude where the empty low-thrust propulsion unit is jettisoned;

3. After a sufficient period of closely observing this high-altitude parking orbit in relation to velocity vector and timing requirements for the Mars transfer trajectory, use the high-thrust engine in one burn to escape earth and establish a Mars-encounter trajectory;

4. Use a second burn of the high-thrust Mars stage, or a second solid propellant rocket, to establish the eccentric capture at Mars encounter.

It is noted that there is an added guidance benefit to be gained by this two-stage, carefully controlled, high parking orbit over escape boost from low earth parking orbit which, because of drag considerations, must be left with haste.

Additional benefits of this approach arise from probable relaxation of insulation specifications for the liquid hydrogen tanks in the low-thrust propulsion stage due to the reduced storage life of the system. Consultation with W. C. Isley of the Goddard Space Flight Center suggests the following reasonable "poodle" engine and tankage constants for such a short-lived (~30 days in earth orbit) mission phase:

$$W_{E,D} = 165 \text{ pounds (four, 1/4-pounds thrust units)}$$

$$C_{T,\text{low thrust}} = 0.15$$

$$I_{sp,\text{low thrust}} = 750 \text{ sec (radioactively heated, cryogenically stored hydrogen) .}$$

Consider an Atlas-Centaur or Titan II/Agena D boost for such a two-stage Mars orbiter mission into a 300 nautical mile, low earth parking orbit. From section II the deliverable payload into this parking orbit is 8800 pounds. The first, low-thrust stage constants are thus

$$C_{T,1} = 0.15$$

$$C_{E,1} = 165/8800 = 0.0188 \text{ .}$$

The engine-tankage constants for the 285 I_{sp} $(I_{sp\text{-high thrust}})$ JPL solid Mars stage are

$$C_{T,2} = 0.177$$

$$C_{E,2} = 0 \text{ ,}$$

as in section II.

In order to compute typical energy requirements for this mission (ignoring plane change requirements as previously), we need to establish a typical value for the required hyperbolic excess speed $V_{\infty,e}$ at earth escape to reach Mars. Reference to Figure 3 reveals this speed requirement to be (assuming coplanar circular orbits for earth and Mars)

$$V_{\infty,e} = V_{perihelion_1} - V_{earth} .$$

The "circular" earth velocity, assuming a radius equal to its semimajor axis, is

$$V_{earth} = \left(\frac{\mu_{sun}}{1.0\ AU}\right)^{1/2} = (0.000296)^{1/2} = 0.0172\ \frac{AU}{solar\ day}$$

(section I). The perihelion velocity in the Hohmann, Earth-Mars transfer ellipse is

$$V_{perihelion_{①}} = \left(\frac{0.000296}{1.262}\right)^{1/2} \left(\frac{2\times 1.262}{1.0} - 1\right)^{1/2} = 0.0189\ AU/solar\ day,$$

from application of Equation 1 at perihelion (earth escape) of this trajectory (section I). Thus

$$V_{\infty,e} = 0.0189 - 0.0172 = 0.0017\ \frac{AU}{day} = 9680\ fps\ ,$$

under the assumptions of this part (Part 1) of the study.

Generalizing this two-stage, two performance mission, let the initial spacecraft weight in the low parking orbit at r_0 be W_0. Let the intermediate staging, high parking orbit be at r_I from the center of the earth. Then, as long as the thrust-to-weight ratio of the low-thrust, first-stage regime is sufficiently low (Reference F1), as it will be for all spacecraft considered here, the ΔV required of the first, low-thrust stage is

$$\Delta V_1 \doteq \left(\frac{\mu_e}{r_0}\right)^{1/2} - \left(\frac{\mu_e}{r_I}\right)^{1/2} , \tag{F3}$$

where subscripts 1 and 2 refer to first and second stages of the mission. The partial ΔV required of the second stage to achieve $V_{\infty,e}$ necessary to reach Mars may be calculated most simply from energy considerations.

If the total velocity at r_I after the first (earth escape-Mars transfer) second-stage burn is $(V_I)_2$ and the velocity at earth escape ($r \to \infty$) is $V_{\infty,e}$, energy conservation in this hyperbolic escape trajectory demands that

$$\frac{(V_I)_2^2}{2} - \frac{\mu_e}{r_I} = \frac{V_{\infty,e}^2}{2} . \tag{F4}$$

From Equation F4

$$\left(V_I\right)_2 = \left[V_{\infty,e}^2 + \frac{2\mu_e}{r_I}\right]^{1/2} . \tag{F5}$$

The ΔV supplied by the first second-stage burn is thus $\left(V_I\right)_2 - (\mu_e/r_I)^{1/2}$. Since the second second-stage burn effects Mars capture, the total second-stage characteristic velocity from the intermediate earth parking orbit is (from Equation F5)

$$\begin{aligned}\Delta V_2 &= \left[V_{\infty,e}^2 + \frac{2\mu_e}{r_I}\right]^{1/2} - \left(\frac{\mu_e}{r_I}\right)^{1/2} + \Delta V(\text{Mars capture}) \\ &= \left(\frac{\mu_e}{r_I}\right)^{1/2}\left\{\left[\left(\frac{V_{\infty,e}}{\left(\mu_e/r_I\right)^{1/2}}\right)^2 + 2\right]^{1/2} - 1\right\} + \Delta V(\text{Mars capture}) .\end{aligned} \tag{F6}$$

From Equation 16, the payload delivered to r_I after first stage separation is

$$\left(W_{PL}\right)_I = W_0\left[M_1\left(1 + C_{T,1}\right) - \left(C_{T,1} + C_{E,1}\right)\right], \tag{F7}$$

where

$$M_1 = e^{-\Delta V_1/gI_{sp,1}} . \tag{F8}$$

Thus the initial weight for the second-stage operations is $\left(W_{PL}\right)_I$. After second stage burns, the payload delivered to the Mars orbit, from Equations 16 and F7, is

$$\begin{aligned}\left(W_{PL}\right)_{Mars} &= \left(W_{PL}\right)_I\left[M_2\left(1 + C_{T,2}\right) - \left(C_{T,2} + C_{E,2}\right)\right] \\ &= W_0\left\{M_1\left(1 + C_{T,2}\right) - \left(C_{T,1} + C_{E,1}\right)\right\}\left\{M_2\left(1 + C_{T,2}\right) - \left(C_{T,2} + C_{E,2}\right)\right\} \\ &= W_0\left\{-M_1\left(1 + C_{T,1}\right)\left(C_{T,2} + C_{E,2}\right) - M_2\left(1 + C_{T,2}\right)\left(C_{T,1} + C_{E,1}\right)\right. \\ &\qquad \left. + M_1 M_2\left(1 + C_{T,1}\right)\left(1 + C_{T,2}\right) + \left(C_{T,1} + C_{E,1}\right)\left(C_{T,2} + C_{E,2}\right)\right\} ,\end{aligned} \tag{F9}$$

where

$$M_2 = e^{-\Delta V_2/gI_{sp,2}} \tag{F10}$$

In terms of the deliverable payload fraction to Mars orbit after the two stage operation, Equation F9 gives

$$(PL)_{F,Mars} = \left(C_{T,1} + C_{E,1}\right)\left(C_{T,2} + C_{E,2}\right) + M_1 M_2 \left(1 + C_{T,1}\right)\left(1 + C_{T,2}\right)$$

$$- M_1 \left(1 + C_{T,1}\right)\left(C_{T,2} + C_{E,2}\right) - M_2 \left(1 + C_{T,2}\right)\left(C_{T,1} + C_{E,1}\right) . \qquad \text{(F11)}$$

Table F1 and Figure F1 give the Mars payload fraction as a function of intermediate parking-staging altitude for this two-stage Mars orbiter mission (from Equation F11, F8, and F10).

It is evident that the optimum performance for this boost system occurs when staging is designed for 10,000-12,000 nautical miles altitude. At this level the Mars payload fraction is about 0.0975, giving a total deliverable orbiter weight of

$$0.0975 \times 8800 = 859 \text{ pounds} .$$

Table F1

Performance of a Two-Stage Mars Eccentric Orbiter Mission as a Function of Intermediate Earth Orbit Staging Altitude.

Earth Orbit			First Stage Performance		Second Stage Performance		Payload Fraction for Mars Orbit, $(P.L.)_{F,Mars}$
Altitude (n.m.)	Radius, r_I (km)	Circular Velocity, $(\mu_e/r)^{1/2}$ (fps)	Velocity Increment, ΔV_1 (fps)	Mission Parameter, M_1	Velocity Increment, ΔV_2 (fps)	Mission Parameter, M_2	
300	6,940	24,900	0	1.000	14,820	0.198	0.055
1,000	8,180	22,900	2,000	0.920	14,000	0.217	0.069
5,500	16,550	16,120	8,780	0.692	11,790	0.276	0.092
7,350	20,000	14,680	10,220	0.655	11,330	0.290	0.095
10,000	24,900	13,150	11,750	0.615	10,910	0.304	0.097
15,450	35,000	11,100	13,800	0.565	10,470	0.320	0.096
20,000	43,500	9,950	14,950	0.537	10,260	0.327	0.094
26,200	55,000	8,850	16,050	0.514	10.090	0.333	0.090

NOTE: 1. Initial weight in 300 n.m. earth orbit: 8800 pounds.

2. First-stage engine: cryogenically-stored, radioisotope-heated hydrogen.

$$W_{E,D} = 165 \text{ lb (four 1/4-lb thrusters)}, \qquad C_{T,1} = 0.15, \qquad I_{sp,1} = 750 \text{ sec.}$$

3. Second-stage engines: JPL "ATS," apogee solids:

$$W_{E,D} = 0, \qquad C_{T,2} = 0.177, \qquad I_{sp,2} = 285 \text{ secs.}$$

4. Mars orbit capture velocity increment: 0.95 km/sec (Mars-synchronous orbiter; 1000 km pericenter altitude).

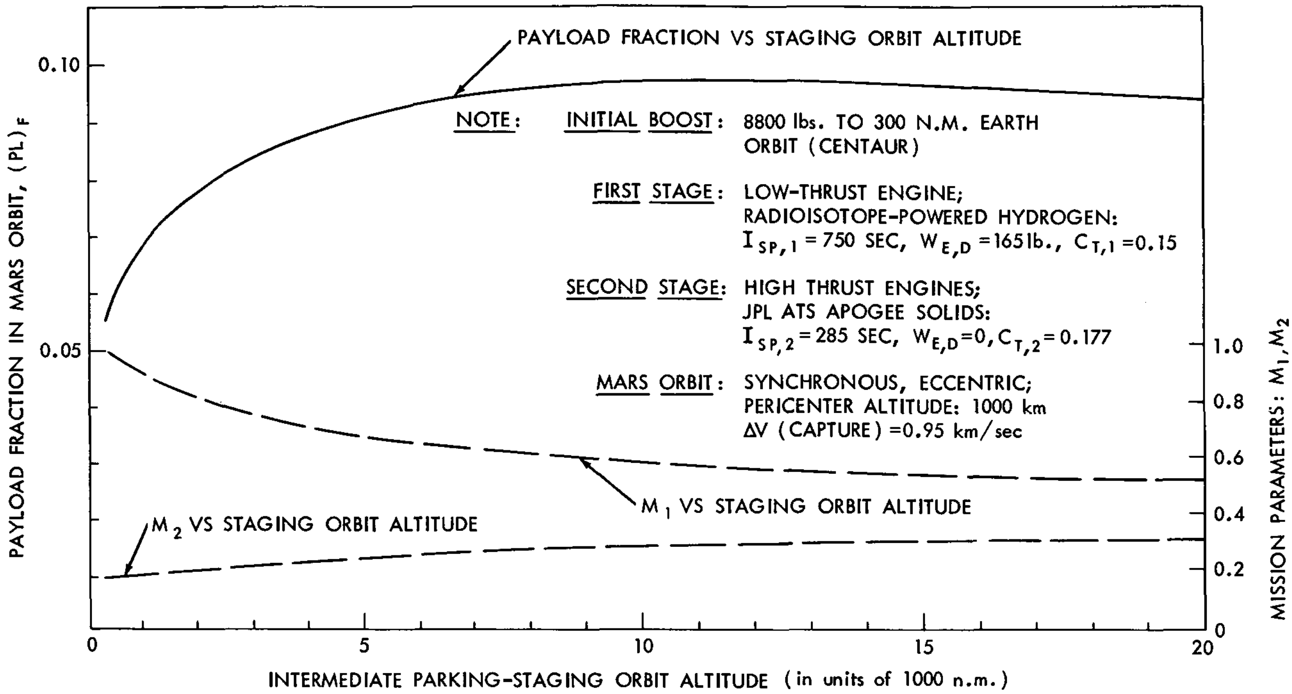

Figure F1—Performance of a low thrust-high thrust boost system for an eccentric Mars orbiter as a function of intermediate earth orbit staging altitude.

In spite of the extra staging involved, the low thrust-high thrust eccentric orbiter is only about 40 pounds heavier out of 820 pounds than the single-stage, high-thrust orbiter. It is evident that the advantage of extra staging in earth orbit is almost entirely dissipated by the energy lost in raising the engine and fuel weight, necessary to reach Mars, to high altitude. This occurs in spite of the high performance of that lifting operation as well.

The results of these calculations are found in Table 1. Similar calculations utilizing this mission profile for a three-stage low thrust-high thrust orbiter mission with the first, earth-escape, solid-stage separable from the spacecraft, show a payload capability of 1020 pounds with an initial Centaur or Titan II/Agena D boost. The optimum high parking orbit prior to low-thrust stage separation is at about 5500 nautical miles altitude in this three-stage mission.

REFERENCES

F1. Duck, K., "An Approximation Method for Determination of Propulsion Requirements Associated with Low Thrust Orbital Transfer in a Central Force Field Under Negligible External Perturbations," GSFC Document X-623-63-117, June 1963.

Appendix G

List of Symbols

a Semimajor axis of an elliptic orbit

C_E Engine deadload fraction

C_T Fuel tankage constant, or factor

c Exhaust velocity of a rocket

g Gravity acceleration at the earth's surface (32.15 ft/sec ^{2})

I_{sp} Specific impulse of a rocket engine (in seconds)

M "Mission parameter," defining the weight-energy efficiency of a mission in terms of its characteristic velocity (ΔV or ΔV_c) and the I_{sp} of the rocket engine

m In Appendix B, the mass of a rocket

PL_f Payload fraction

r Distance from a central attracting body

r_a Apocenter distance (farthest) from a central attracting body

r_p Pericenter distance (nearest) from a central attracting body

$\bar{r}$ Optimum radius for a circular orbit of a planet, achievable by a one-impulse capture maneuver

s/c Spacecraft

T_e Thrust of a rocket engine

T_s Period of satellite orbit about a central attracting body

t Mission, or burn, or engine "on" time

V Velocity of the spacecraft or planet

V_a Velocity at apocenter

V_c Circular orbital velocity

V_p Velocity at pericenter

V_∞ Velocity at a large distance from a central attracting body, with respect to that body

$V_{\infty,M}$ Relative velocity between Mars and the approaching spacecraft at or near Mars encounter

W Weight (in pounds, at the earth's surface)

Δ, d Small increment, a differential increment

Δv Velocity increment

Δv_c Velocity increment, the characteristic (total) velocity increment of a mission or mission phase

μ Gaussian gravity constant of a central attracting body

NASA-Langley, 1967